ADA216418

UNCLASSIFIED

SECURITY CLASSIFICATION OF THIS PAGE

REPORT DOCUMENTATION PAGE

Form Approved
OMB No. 0704-0188

1a. REPORT SECURITY CLASSIFICATION Unclassified	1b. RESTRICTIVE MARKINGS
2a. SECURITY CLASSIFICATION AUTHORITY	3. DISTRIBUTION/AVAILABILITY OF REPORT Approved for public release; distribution unlimited.
2b. DECLASSIFICATION/DOWNGRADING SCHEDULE	
4. PERFORMING ORGANIZATION REPORT NUMBER(S) HDL-TM-89-6	5. MONITORING ORGANIZATION REPORT NUMBER(S)
6a. NAME OF PERFORMING ORGANIZATION Harry Diamond Laboratories 6b. OFFICE SYMBOL (If applicable) SLCHD-NW-TN	7a. NAME OF MONITORING ORGANIZATION
6c. ADDRESS (City, State, and ZIP Code) 2800 Powder Mill Road Adelphi, MD 20783-1197	7b. ADDRESS (City, State, and ZIP Code)
8a. NAME OF FUNDING/SPONSORING ORGANIZATION U.S. Army Laboratory Command 8b. OFFICE SYMBOL (If applicable) AMSLC	9. PROCUREMENT INSTRUMENT IDENTIFICATION NUMBER
8c. ADDRESS (City, State, and ZIP Code) 2800 Powder Mill Road Adelphi, MD 20783-1145	10. SOURCE OF FUNDING NUMBERS PROGRAM ELEMENT NO. 6.21.20 / PROJECT NO. / TASK NO. / WORK UNIT ACCESSION NO.
11. TITLE (Include Security Classification) On Multiple Edge Diffraction and Multiple Reflections of Microwaves over Terrain	
12. PERSONAL AUTHOR(S) Albert G. Gluckman	
13a. TYPE OF REPORT Final 13b. TIME COVERED FROM Oct 86 TO Nov 88	14. DATE OF REPORT (Year, Month, Day) November 1989 15. PAGE COUNT 81
16. SUPPLEMENTARY NOTATION AMS code: P612120.140, HDL project: 2E6821	

17. COSATI CODES			18. SUBJECT TERMS (Continue on reverse if necessary and identify by block number)
FIELD	GROUP	SUB-GROUP	Microwave diffraction, microwave reflection, microwave propagation over terrain, microwave edge diffraction, knife edges, muiltiple diffracting knife edges, diffracting ray paths.
15	02		
20	06		

19. ABSTRACT (Continue on reverse if necessary and identify by block number)

This report describes a computer model which is an extension of the method of Deygout-Meeks for computing power density on target from microwaves propagated over terrain. The Meeks procedure is concerned with broadcast/isotropic radiation at very high frequencies (vhf) and accounts for the effects of diffraction across a single knife edge, as well as ground reflections of microwaves over electrically interactive terrain at low incidence angles of transmission. This model is extended to describe either broadcast vhf radiation or beamed microwaves that are diffracted over two edges.

20. DISTRIBUTION/AVAILABILITY OF ABSTRACT ☒ UNCLASSIFIED/UNLIMITED ☐ SAME AS RPT. ☐ DTIC USERS	21. ABSTRACT SECURITY CLASSIFICATION Unclassified
22a. NAME OF RESPONSIBLE INDIVIDUAL Albert G. Gluckman	22b. TELEPHONE (Include Area Code) (202) 394-3060 22c. OFFICE SYMBOL SLCHD-NW-TN

DD Form 1473, JUN 86 *Previous editions are obsolete.*

SECURITY CLASSIFICATION OF THIS PAGE
UNCLASSIFIED

Contents

Appendices

Appendices

Page

Figures

Executive Summary

In response to a recommendation stemming from an earlier report* that "the knife edge model be extended to include multiple knife edges," this study develops, as a special case, a computer program model of microwave diffraction over two edges/hills that are situated on a flat earth.

In summary, the following has been accomplished in this report:

An extension is made of the Meeks knife-edge method for computing power density on target, in order to consider double diffraction. Whereas Meeks' method (which itself is an extension of Deygout's 1966 simplification of diffraction computations for the Kirchhoff knife-edge theory) models the broadcast of microwaves over a single knife edge, the method described here models, at the discretion of the user, either isotropically broadcast or anisotropically beamed microwave radiation over two knife edges.

In order to make this extension, one constructs a set of uniquely described ray paths from the source antenna to the sink antenna. The model describes double diffraction of microwaves across electrically interactive terrain with ground reflections at low incidence angles. This method can be further extended for diffraction over more than two edges.

Albert G. Gluckman, The Lobing Structure of Microwave Radiations due to Reflection and Diffraction from Terrain (U), Harry Diamond Laboratories, HDL-TM-86-10 (September 1986). (CONFIDENTIAL)

1. Introduction

Suppose a ray path of a microwave train is diffracted by two knife edges which are set on a flat earth. How can we determine by how much or by how many decibels the power level is diminished by the diffraction? And if interference occurs between this ray and a direct ray, how does this interference affect the power level of the train of microwaves? Further, if reflection occurs at one, two, or three points that are separated by the knife edges (see fig. 1), how much power density of the train of microwaves is lost to eddy currents in the conductive soil?

Apropos both the computational characteristics and the theoretical underpinnings/foundations of propagation models, the following question comes to mind. How can the reduction in power level for a single knife edge [1-6]* be extended to apply to the problem of determining the reduction in power level for two knife edges, for all reflection path geometries that are encountered?

The purpose of this report is to show how this may be accomplished. The FORTRAN program to do this (called DOUBLEDGE) is shown in appendix B. It can handle the propagation of either broadcast radiation at vhf or of beamed microwaves which have much higher frequencies.

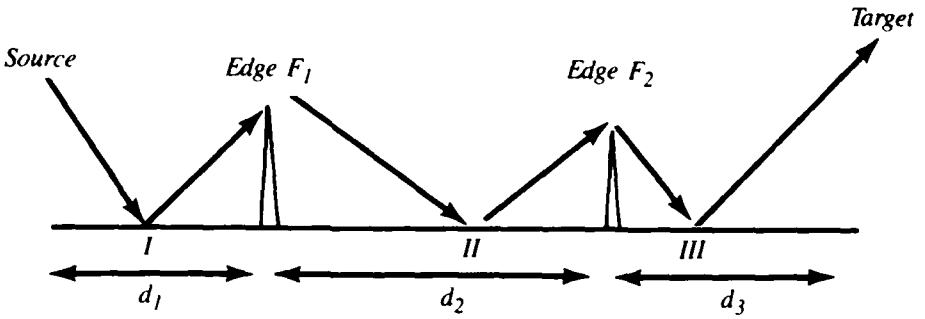

Figure 1. Knife-edge diffraction and reflection for example of two diffractions and three reflections.

I: 1st point of reflection on terrain
II: 2d point of reflection on terrain
III: 3rd point of reflection on terrain
F_1: Edge of 1st diffraction
F_2: Edge of 2d diffraction

*References are listed at the end of the main body of text (p 23).

The report first discusses propagation of the direct ray, next the indirect ray, and then the application of the double-knife-edge model, ending with a discussion of the results.

Appendix A shows the diffractive ray-path geometries for two knife edges, appendix B is a listing of the FORTRAN computer program of the model, and appendix C is a program listing which was used to extract the data subset for making the plots shown in appendix D.

The plots in appendix D show the change in power density at the target, expressed in decibel scale (relative to free space level of 0-dB decrement), versus target height. The plots show a good agreement of accepted theory with the results from the model. Because of its simplicity, this method takes little computer time.

Appendix E contains plots of single diffraction and double diffraction of microwaves. Some of these plots are used to show how power density at the target after single diffraction will compare to power density at the target after double diffraction. Some other plots in appendix E show how, by changing emitter height, battlefield saturation by radiation can be enhanced.

Appendix F shows a plot comparing a theoretically derived curve for two diffractions over electrically interactive terrain with a curve that is derived from actual propagation data collected in the field from measurements. These propagation data are taken with respect to the transmitter on an azimuth to a location called Forest Hill.

Appendix G shows a plot comparing a theoretically derived curve for a single diffraction over terrain (using the KNIFEDGE program) to a curve prepared from field measurement data for two diffractions over terrain. These propagation data are taken with respect to the transmitter on an azimuth to Forest Hill.

2. Direct Ray Path

There are three possible geometries to describe the clearance of the direct ray path over two knife edges. The three geometries depend on whether

the heights of the two knife edges, F_1 and F_2, are as $F_1 < F_2$, as $F_1 > F_2$, or as $F_1 = F_2$. These geometries are pictured in figure 2.

With sufficient distance above the knife edges, relative to wave length, these ray paths exhibit no diffraction. They are called the direct ray paths, or the direct rays.

Let us consider knife-edge heights F_1 and F_2; the distances d_1, d_2, and d_3 downrange; the height of the transmitter, z_1; and the height of the target, z_2, as illustrated in figure 2. From these three diagrams in figure 2, a logical choice can be made as to which path geometry is appropriate. This is done by a testing algorithm which is based on (1) the sign and magnitude of the slope angles of the paths over the edges and on (2) whether F_1 is greater than, equal to, or less than F_2.

From figure 3, the slope angles are

$$\alpha_1 = \tan^{-1}\left[(F_1 - z_1)/d_1\right]$$

and

$$\alpha_2 = \tan^{-1}\left[(F_2 - z_1)/(d_1 + d_2)\right] \quad .$$

So, if

$$F_1 < F_2 \text{ and } \alpha_1 < \alpha_2 \ ,$$

the direct path has F_2 as its edge of closest approach. In this case, the normalized electric amplitude A_{12} associated with the Fresnel diffraction of an assumed wave over F_2 is calculated. If

$$F_1 < F_2 \text{ and } \alpha_1 \geq \alpha_2 \ ,$$

or if,

$$F_1 > F_2 \text{ and } \alpha_1 \geq \alpha_2 \ ,$$

the direct path has F_1 as its edge of closest approach. In this case, the normalized electric amplitude A_{11} associated with the Fresnel diffraction of an assumed wave over F_1 is calculated.

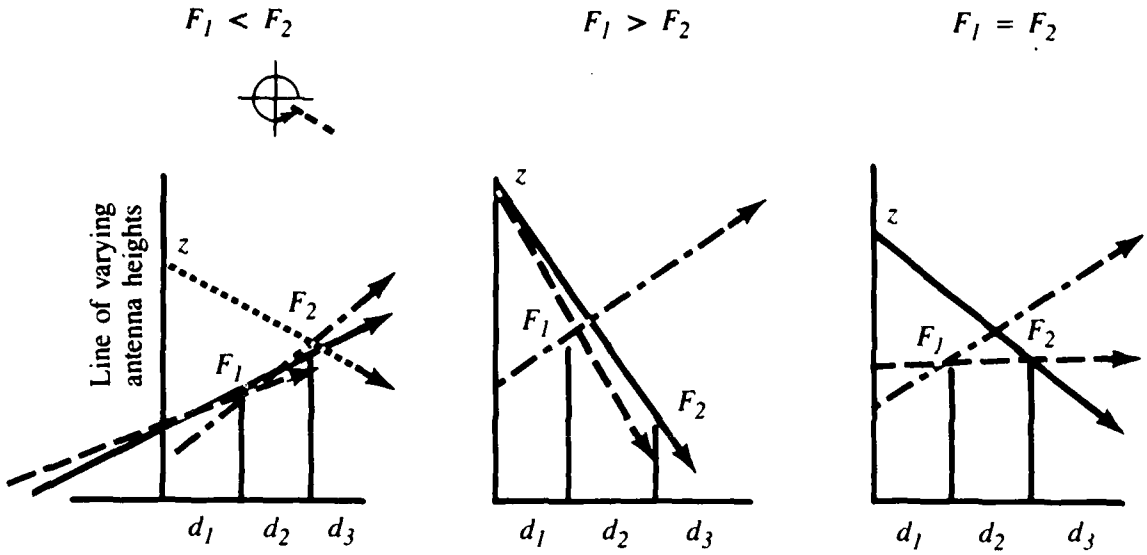

Figure 2. Clearance of direct ray path over knife edges F_1 and F_2.

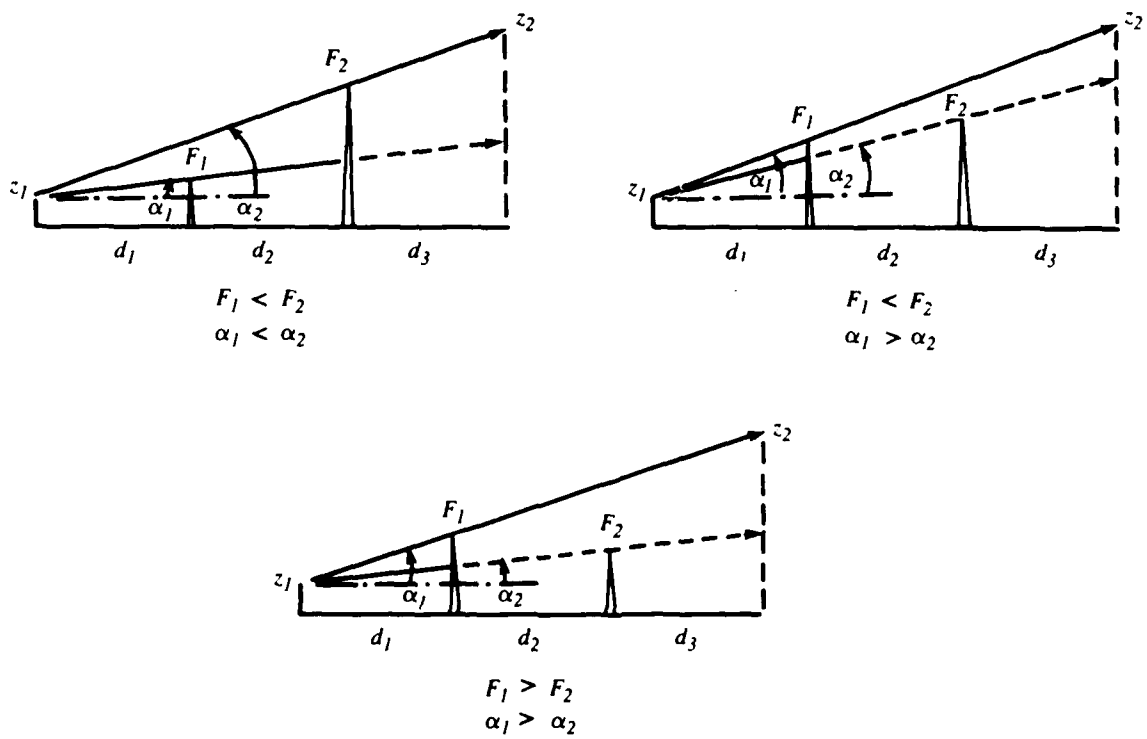

Figure 3. Geometry for determining direct path over edge F_1 or F_2, based on slope angle and ray path and relative heights of F_1 and F_2.

The normalized electric amplitudes, A, of these direct ray paths (as well as the indirect paths discussed in the next section, which experience reflection as well as diffraction) are computed with the aid of the Cornu spiral approximations for the Fresnel integrals.

3. Indirect Ray Path

The indirect ray path is a path along which a microray experiences diffraction from one or more knife edges, as well as reflection from the ground/terrain. A microray is a ray at microwave frequency. The theory of ray optics was applied by Deygout, and later Meeks, to the problem of microwave propagation from a point-source emitter.

The ray path emanating from the point-source microwave transmitter is hypothesized to be a continuous signal. This signal can be diffracted by intervening hills/ridges, as well as reflected by flattened terrain profile features. Interference patterns arise when these diffracted and reflected rays interfere with the direct rays.

This method for determining diffraction over two geometries takes into account the diminution of electric amplitude that is associated with each ray path geometry.

From figures 2 and 4, it can be seen that reflection of a ray can occur

on d_1 or on d_2 or on d_3 separately;
or on d_1 and d_2, or on d_1 and d_3, or on d_2 and d_3 conjointly;
or on d_1 and d_2 and d_3 in concert.

Furthermore, it is evident that diffraction can occur at F_1 or at F_2 or at both F_1 and F_2, together with any of the possibilities of reflection just mentioned. This means that a total of 14 ray-path geometries are possible for an indirect ray path.

Another level of complication in the theory is that the target height is raised in discrete intervals, so that for each increase, the reflection points alter or shift in position on the terrain, and the grazing angles change. Since the reflecting electric ray interacts electrically with the terrain, eddy currents are formed in the soil at the point of reflection, and electric energy is lost in the soil in the form of Joule heat. This means that the resulting

reflected electric microray has a diminished amplitude. The reflection coefficient depends upon permittivity (which is the dielectric constant) of the soil, wave length, conductivity of the soil (in siemens), and the grazing angle (in radian measure). Figure 4 shows how to determine the respective grazing angles *PSI*1, *PSI*2, and *PSI*3 of a ray over terrain regions d_1, d_2, and d_3, respectively.

In the computer program (with fig. 3 in mind), *CTV* is the vertical polarization reflection coefficient and *CTH* is the corresponding horizontal polarization reflection coefficient. The reflection coefficient determines the diminution (or reduction) in the (normalized) electric amplitude of the ray, after reflection on the ground. This means that after reflection, there is a corresponding reduction in the eventual power density output at target from this ray path.

The subroutine FRESNL (in app B) computes the reflection coefficient. The FORTRAN parameter ANG in subroutine FRESNL takes the values *PSI*1, *PSI*2, or *PSI*3 of the grazing angles in radians. *PSI*1, *PSI*2, and *PSI*3 are the grazing angles over d_1, d_2, and d_3, respectively.

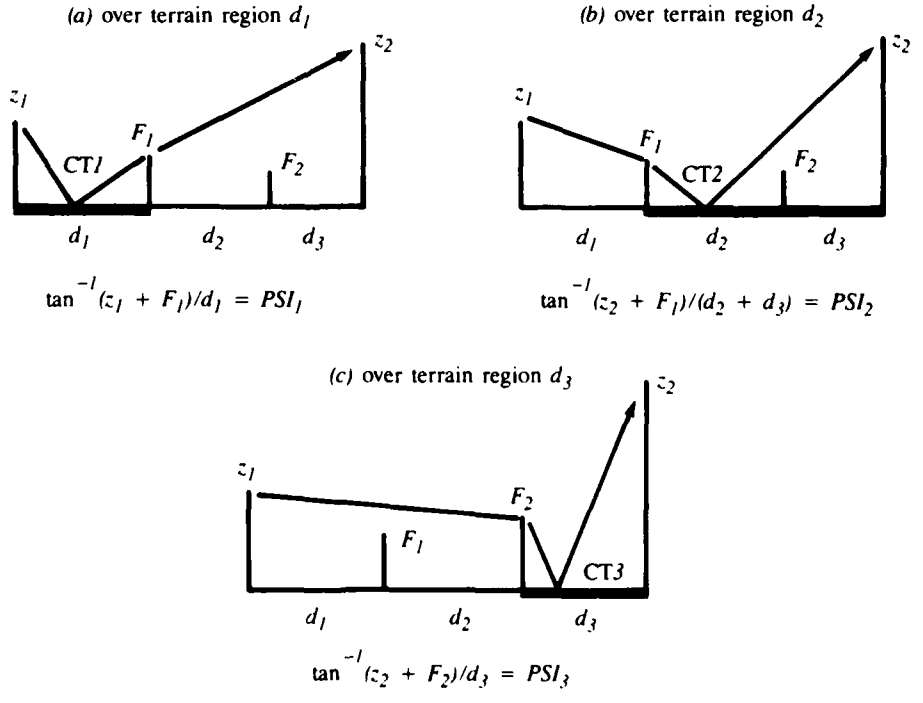

Figure 4. Ray-path geometry for determining grazing angles over terrain regions (needed for computing reflection coefficients CT_i, where i = 1, 2, or 3).

For either horizontally or vertically polarized microwaves, the calculated Fresnel reflection coefficient (*CTH* or *CTV*) and the ground reflectivity $REFL_i$ (in FORTRAN computer code) are multiplied together in one-to-one correspondence with the appropriate terrain interval d_i. This means that

$$CT_i = \left\{ \begin{matrix} CTH \\ \text{or} \\ CTV \end{matrix} \right\} \times REFL_i \quad , \text{ where } i = 1, 2, \text{ or } 3 \quad ,$$

and CT_i is the amended reflection coefficient.

In order to distinguish beamed/anisotropic propagation at microwave frequency from broadcast/isotropic propagation at vhf, the computer program relies on the data input of either "anisotropic" or "isotropic." If a beam is formed, a corresponding high-frequency input is necessary in order to satisfy the physical requirements of the generic theory. Just as in the KNIFEDGE program [7] of the diffraction of a microray (or its associated microwave) caused by a single edge, so too, in this DOUBLEDGE program model is the nonisotropic radiator incorporated into the theory by considering the on-axis ray of the antenna as the direct ray and the off-axis ray as the reflected ray. The magnitude of the reflected ray is less than that of the direct ray by an E-field reduction factor:

$$E_R = GRdB = 10^{(G-C)/20} \quad ,$$

where G is the gain of the antenna in decibels and C is the on-axis antenna gain. In the isotropic case, gain due to directivity is not considered.

Corresponding to each of the two knife edges F_1 and F_2, there is a clearance parameter of a first Fresnel zone. For edge F_1, this is

$$\Delta_{12} = \sqrt{\frac{\lambda d_1 d_2}{d_1 + d_2}}$$

and for F_2, this is

$$\Delta_{23} = \sqrt{\frac{\lambda d_2 d_3}{d_2 + d_3}} \quad .$$

For the edge F_1, the argument u of the Fresnel integrals

$$C(u) = \int_0^u \cos \frac{\pi}{2} u^2 \, du \text{ and } S(u) = \int_0^u \sin \frac{\pi}{2} u^2 \, du$$

when multiplied by the factor $2^{-1/2}$ forms the ratio of the clearance parameter Δ of the direct ray over or through (if negative clearance below) the knife edge F_1 expressed in units of clearance of the first Fresnel zone Δ_{12}. Thus $u = \Delta\, 2^{1/2}/\Delta_{12}$.

On the other hand, for the edge F_2, $u2^{-1/2}$ is the ratio of the clearance parameter Δ of the direct ray over or through (if negative clearance below) the knife edge F_2 expressed in units of clearance of the first Fresnel zone. Thus $u = \Delta\, 2^{1/2}/\Delta_{23}$.

Clearance parameters Δ_{12}, corresponding to edge F_1, are calculated for each of the seven generic indirect ray paths over F_1, and this calculation is iterated for each change that occurs due to the stepping of the target height as it gains altitude. Likewise, clearance parameters Δ_{23}, corresponding to edge F_2, are calculated for each of the defined seven generic indirect ray paths over F_2.

The choice of the direct ray path may be taken over either knife-edge F_1 or F_2, but this choice is decided by the method that is described in section 2. If knife edge F_1 is the one of closest approach to the ray, yet far away enough not to contribute any diffractive effects (i.e., the bending of the ray due to the presence of the knife edge), the normalized electric amplitude A_{11}, corresponding to F_1 is calculated. If, on the other hand, F_2 satisfies this condition, the normalized electric amplitude A_{12} is calculated. Note that in the notation A_{11} and A_{12}, the first subscript, 1, refers to the direct ray; the second subscript refers to either edge F_1 or F_2.

In more detail, normalized electric field amplitudes for each of the direct rays over F_1 or F_2 are computed independently; and this is true for all computations involving the indirect rays as well. The choice of either direct ray over F_1 or over F_2 is made by the decision algorithm based on slope and the relative heights of edges F_1 and F_2 that is described in figure 3 of section 2. There can only be one direct ray.

Likewise, normalized electric field amplitudes A_{ij} corresponding to each of the 14 remaining generic indirect ray paths are computed in a stepwise fashion for each iteration, as the target height increases step by step to the maximum designated height. The electric field contributions for all paths at a particular height are summed for their total field value. The normalized electric amplitudes A_{ij}, where $i = 1$ through 8 (corresponding to path), and $j = 1$ or 2 (corresponding to edge F_1 or F_2), is derived from the equation

$$A_{ij}\sqrt{2} = (C + 0.5)^2 + (S + 0.5)^2 \quad ,$$

where

$$0 \leq A_{ij} \leq 1 \quad .$$

All A_{ij} values are derived independently of each other. For the case of the 14 paired indirect-ray-path geometries, the electric amplitudes of the seven pairs of ray paths (shown in app A) are combined as

$$A_{21}A_{22},\ A_{31}A_{32},\ A_{41}A_{42},\ A_{51}A_{52},\ A_{61}A_{62},\ A_{71}A_{72},\ A_{81}A_{82}$$

for all iterations on target height. These products of normalized electric amplitudes reduce the available energy on target, because of diffractive loss due to the bending of rays into the shadow region behind the hills.

Because the values of the amplitudes A_{ij} theoretically lie between 0 and 1 (except that in actual practical use numerical error may cause this condition to be sometimes violated to some extent), they act to diminish the power density of the electric field corresponding to each ray path associated with this diffracted foward scattering. The combined effect of the pairwise products of these amplitudes (which may be called product

amplitudes), as shown just above, are a measure of the reduction in power density at the target due to the diffraction induced by both knife edges F_1 and F_2.

The expression CE_i is a complex number expressing the magnitude (amplitude) and the phase lag angle of each contribution of the electric field corresponding to each iteration of the target height, for each generic path. The total magnitude for each field contribution is expressed as $A_{i1}A_{i2}$ multiplied by the appropriate combination of reflection coefficients, CT_i, and by the gain reduction factor, E_R, to account for the beam concentration of microwave radiation.

The phase lag angle B, where

$$B = \tan^{-1}\left(\frac{S+0.5}{C+0.5}\right) + \frac{k\pi}{4} \quad , \; k = -1 \text{ or } 3 \; ,$$

is due to the difference between the phase angle of the reflected ray and direct ray, at target, and this is a consequence of the differences in the path lengths of the direct and indirect (reflected) rays. Therefore, the relative power density at target in decibel units, relative to propagation in free space is

$$20 \log C E_1 + \sum_{i=2}^{8} C E_i \; ,$$

where CE_1 is the complex form for the electric contribution $A_{11}\, e^{B\sqrt{-i}}$ or $A_{12}\, e^{B\sqrt{-i}}$ for the direct ray; and CE_i, i = 2 to 8, is the complex form of the electric contribution for each of the paired generic indirect ray paths, expressed as

$$C E_{22} = A_{21} A_{22}\, e^{B\sqrt{-1}}\, e^{-2\pi\Delta R_{21}/\lambda} e^{-2\pi\Delta R_{22}/\lambda}\, \Gamma_1\, E_R$$

$$C E_{32} = A_{31} A_{32}\, e^{B\sqrt{-1}}\, e^{-2\pi\Delta R_{31}/\lambda} e^{-2\pi\Delta R_{32}/\lambda}\, \Gamma_2\, E_R$$

$$C E_{42} = A_{41} A_{42}\, e^{B\sqrt{-1}}\, e^{-2\pi\Delta R_{41}/\lambda} e^{-2\pi\Delta R_{42}/\lambda}\, \Gamma_1 \Gamma_2\, E_R$$

$$C E_{52} = A_{51} A_{52}\, e^{B\sqrt{-1}}\, e^{-2\pi\Delta R_{51}/\lambda} e^{-2\pi\Delta R_{52}/\lambda}\, \Gamma_3\, E_R$$

$$C E_{62} = A_{61} A_{62} e^{B\sqrt{-1}} e^{-2\pi\Delta R_{61}/\lambda} e^{-2\pi\Delta R_{62}/\lambda} \Gamma_2 \Gamma_3 \; E_R$$

$$C E_{72} = A_{71} A_{72} e^{B\sqrt{-1}} e^{-2\pi\Delta/\lambda} e^{-2\pi\Delta R_{72}/\lambda} \Gamma_1 \Gamma_3 \; E_R$$

$$C E_{82} = A_{81} A_{82} e^{B\sqrt{-1}} e^{-2\pi\Delta R_{81}/\lambda} \cdot e^{-2\pi\Delta R_{82}/\lambda} \Gamma_1 \Gamma_2 \Gamma_3 \; E_R$$

where the amended reflection coefficients $CT_i = \Gamma_i$ each correspond to their associated terrain region d_i.

The normalized electric amplitudes A_{i1} and A_{i2} (i = 2 through 8) refer to diffraction at edges F_1 and F_2, respectively, for all pairs of ray path geometries that are described in figure A-1 of appendix A.

4. Application of the DOUBLEDGE Computer Program

Figure 5 shows how terrain with two prominent features/hills can be pictured for the particular example where the transmitter, T, is set up on a high hill overlooking the predominantly downhill terrain. Two large hills lie between the transmitter, T, and the target, S, located downrange. The intervening hilltops are located at positions (X_4, Y_4) and (X_6, Y_6). The line X_1X_2 is parallel to sea level in the flat earth model. The terrain distance and height parameters are referenced to the lowest position above sea level, X_2, in the same manner as this was done by Gluckman [7] in his KNIFEDGE computer model of a microwave beam that is diffracting over a single hill/ridge. The microwave targeting position lies above position X_2 at location ground zero.

With the use of the appropriate data derived from actual measured field transmissions and receptions, this doubly diffractive model with attendant/accompanying reflections can be tested for its accuracy in representing actual physical conditions of terrain, polarity of the wave, and frequency, with respect to the measured signal strength.

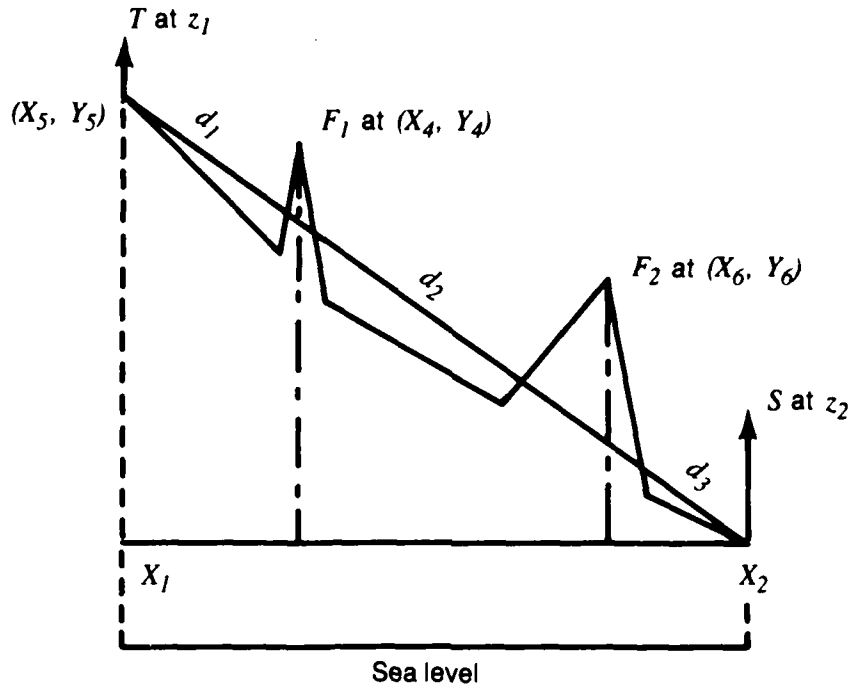

Figure 5. Double-knife-edge model over terrain.

5. Discussion of Results

By the expedient of raising or lowering the height of the high-power microwave transmitter, one can alter the elevations of the power density lobes. This would result in increasing the coverage of electric energy on targets over or about the position of ground zero. This procedure would change the amount of diffracted energy in the umbra/shadow which is below the line of sight, thereby increasing the energy level of radiation that can be placed on a target behind a hill. The method developed in this report to determine power loss resulting from two diffractions, for ray paths reflecting from electrically interactive terrain, can be extended to the case of diffraction occurring over n edges.

5.1 Comparison of Power Loss of Double Versus Single Diffraction

In comparing the plots of appendix E in

figure E-1, where $D1$ = 2500 m and $D2$ = 5000 m,

figure E-2, where $D1$ = 3750 m and $D2$ = 3750 m, and

figure E-3, where $D1$ = 5000 m and $D2$ = 2500 m,

all other electric and geometric terrain parameters remaining the same, one makes the following observations.

In all three plots, power loss due to double diffraction is greater than for single diffraction, and the double-diffraction power loss curves asymptotically follow the single diffraction curves for dB down (loss). Above line of sight at target, the power loss curves for double- and single-edge diffraction intertwine with each other in a dampening oscillation through/at the 0-dB region. It is noticed that when the single knife edge is closer to the emitter, the power loss curves for double- and single-edge diffraction show a closer asymptotic approach, as shown in figure E-1. As the single knife edge arrives at the midpoint of the target range, the two curves fall further apart, nevertheless maintaining their parallel character, as shown in figure E-2. This characteristic is further accentuated as the single knife edge approaches the target, as shown in figure E-3. In all three cases, however, the power loss curve at target, of diffraction due to two knife edges, exhibits spikes of high loss, but these spikes are very narrow. However, these spikes appear as natural extensions of the oscillations of the single-knife-edge power loss curves. The tails of these isolated spikes may show a power loss at their corresponding height above the terrain, as much as 30 to 35 dB less than power loss due to single-edge diffraction.

5.2 Comparison of Power Loss of 3-m Versus 6-m Antenna Height

Diffraction due to two knife edges. Plot E-4 (see app E) shows that power loss is greater for an emitting antenna placed at a height of 3 m than at 6 m. Note that in both cases, all the electric and geometric terrain parameters remain the same.

Diffraction due to a single knife edge. In comparing the plots of appendix E in

figure E-5, where $D1$ = 2500 m and $D2$ = 5000 m,

figure E-6, where $D1$ = 3750 m, and $D2$ = 3750 m,

figure E-7, where $D1$ = 5000 m and $D2$ = 2500 m,

all other electric and geometric terrain parameters remaining the same, one makes the following observation.

Where the knife edge is at first closer to the emitter, and moves to a location midway between the emitter and the target, as shown in figures E-5 and E-6, the power loss is greater for an antenna set at a 3-m height than for an antenna situated higher, at a 6-m height above the terrain. Both power loss curves, however, show parallelism, as if they were shifted apart by a horizontal translation along the abscissa. At the 0-dB vertical region of the plot (at free space propagation on the decibel scale considered as a reference-value/origin, against which to measure propagation over terrain), the two power loss curves intertwine in a dampening oscillation as altitude of the target increases (i.e., as altitude increases, the dampening of the power loss oscillation increases).

Where the knife edge is set farther away from the emitter, and therefore closer to the target, as shown in figure E-7, the difference in diffractive power loss due to changing the emitter-antenna height from 3 to 6 m is lost.

5.3 Verification of the DOUBLEDGE Diffraction Theory with Collected Field Data

In November 1979 and February 1980, M. L. Meeks conducted an on-site measurement survey of electric field output (or equivalently, of power output) for the Lincoln Laboratory of the Massachussetts Institute of Technology (MIT). His transmitter was a vhf omnidirectional radio station, used as an aircraft navigation aid, situated on a hilltop about 80 km west of Boston, MA. This station transmitter propagated a signal at 110.6 MHz, with an omnidirectional pattern which was symmetrical in azimuth. The polarization was horizontal.

The survey measurements were made onboard a vertically descending helicopter. The receiving antenna was a horizontal dipole located under the fuselage. The effect of antenna gain due to elevation was ignored. In the horizontal plane, however, gain was isotropic, that is, the same in all directions. Additional details of these survey measurements are available elsewhere [4,5].

Lincoln Laboratory supplied Harry Diamond Laboratories (HDL) with raw digital measurement data from the azimuthal propagation path, along

which (for our study) the signal was measured above the terrain at the target. This path was from the transmitter to a location called Forest Hill. Two measurements were made independently for this path across the terrain. This particular path was chosen because it displayed two prominent diffractive hills across which the signal was propagated.

The forest population consisted of a mix of evergreen and deciduous trees which had lost their leaves for the winter season.

At HDL, the two independent aggregates of signal measurements were averaged at 5-m interval heights for this path from the transmitter to the Forest Hill location.

The curve shown in plot F-1 of appendix F, describing an averaged data measurement set, was compared with the theoretically derived curve for this azimuth. As can be seen, the results are very favorable, and the closeness of fit verifies the validity of the "doubledge" theory. It is recommended that a statistical study be made of the characteristics of this closeness.

In the computations of the theoretically derived curves, care was taken to calculate the scattering/reflectivity coefficient, ρ, for each plot, in accordance with theory. To this end, the formula

$$\rho_{av}^2 = e^{-(\Delta\phi)^2} \; ; \; \Delta\phi = \frac{4\pi\Delta h \sin\psi}{\lambda}$$

was applied, where

ϕ is phase lag angle,

$\Delta\phi$ is phase difference between two rays reflecting from the surface,

Δh is standard deviation of normal distribution of hill heights,

ψ is the grazing angle, and

λ is wave length.

5.4 Comparison of Theoretically Derived Power Density Loss for Single Diffraction with Data for Diffraction over Two Peaks

In appendix G, plot G-1 shows the theoretically derived curve of power density loss due to diffraction over one peak (using the four-ray-path-theory computer program describing diffraction over a single edge, with reflections on electrically interactive terrain [3,7]) compared to field measurement data for signal transmission over two peaks.

5.5 Plots for Doubly Diffracted Horizontally Polarized Microwaves Based on Theory and the Application of Program DOUBLE_PLOT

It should be noted that appendix D shows plots of power density at target heights downrange for doubly diffracted horizontally polarized microwaves.

The computer program DOUBLE_PLOT, listed in appendix C, sets up the numerical power density values (as the abscissa) versus target heights (as the ordinate) for each plot in appendices D through G.

Literature Cited

1. M. Littleton Meeks, *A Propagation Experiment Involving Reflection and Diffraction*, Massachusetts Institute of Technology (MIT) (26 October 1981). ADA108644

2. M. Littleton Meeks, *A Propagation Experiment Combining Reflection and Diffraction*, IEEE Trans. Antennas Propag., AP-30, No. 2 (March 1982), pp 318-321.

3. M. Littleton Meeks, *Radar Propagation at Low Altitudes*, Artech House, Inc., Dedham, MA (1982).

4. M. Littleton Meeks, *VHF Propagation over Hilly, Forested Terrain*, IEEE Trans. on Antennas and Propag., AP-31, No. 3 (May 1983), pp 483-489.

5. M. Littleton Meeks, *VHF Propagation over Hilly, Forested Terrain*, Massachusetts Institute of Technology (MIT) (April 1982). ADA115746

6. M. Littleton Meeks, *VHF Propagation Near the Ground: An Initial Study*, Massachusetts Institute of Technology (MIT) (26 October 1982). ADA122498

7. Albert G. Gluckman, *The Lobing Structure of Microwave Radiations due to Reflection and Diffraction from Terrain* (U), Harry Diamond Laboratories, HDL-TM-86-10 (September 1986). (CONFIDENTIAL)

Appendix A. — Picturing Diffractive Ray-Path Geometries for Two Knife Edges

The following diagrams represent unique ray paths associated with each of their normalized electric amplitudes A_{jk}, where $j = 2,..., 8$, and $k = 1, 2$.

Note that in this appendix, each pair of ray path diagrams (designated A_{i1} and A_{i2}) shown in figure A-1 describes the diffraction that occurs when a ray passes over two knife edges. The diagrams of the figure give insight first to the diffractive influence caused by the passage of the ray over peak F_1 and, second, to the diffractive influence caused by passage of the ray over peak F_2. To each diagram (A_{i1} or A_{i2}; $i = 2, ..., 8$) there corresponds a version of the algebraic expression for computing the total indirect ray path amplitude $A_{i1}A_{i2}$. The notation designating the diagrams of the figure and the notation designating the respective amplitudes are the same.

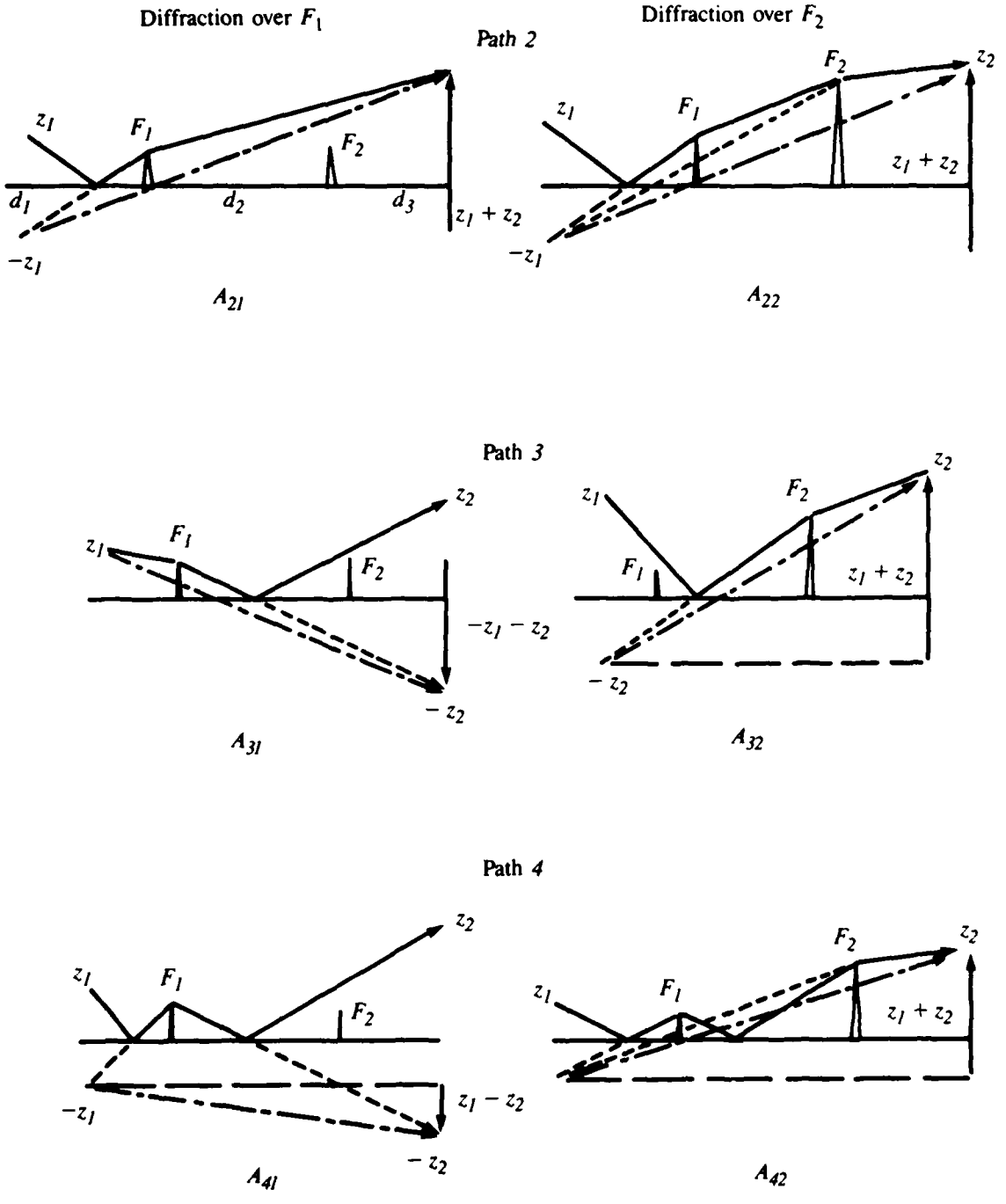

Figure A-1. Indirect ray paths and their corresponding normalized electric amplitudes (note: path 1 is the direct ray).

APPENDIX A

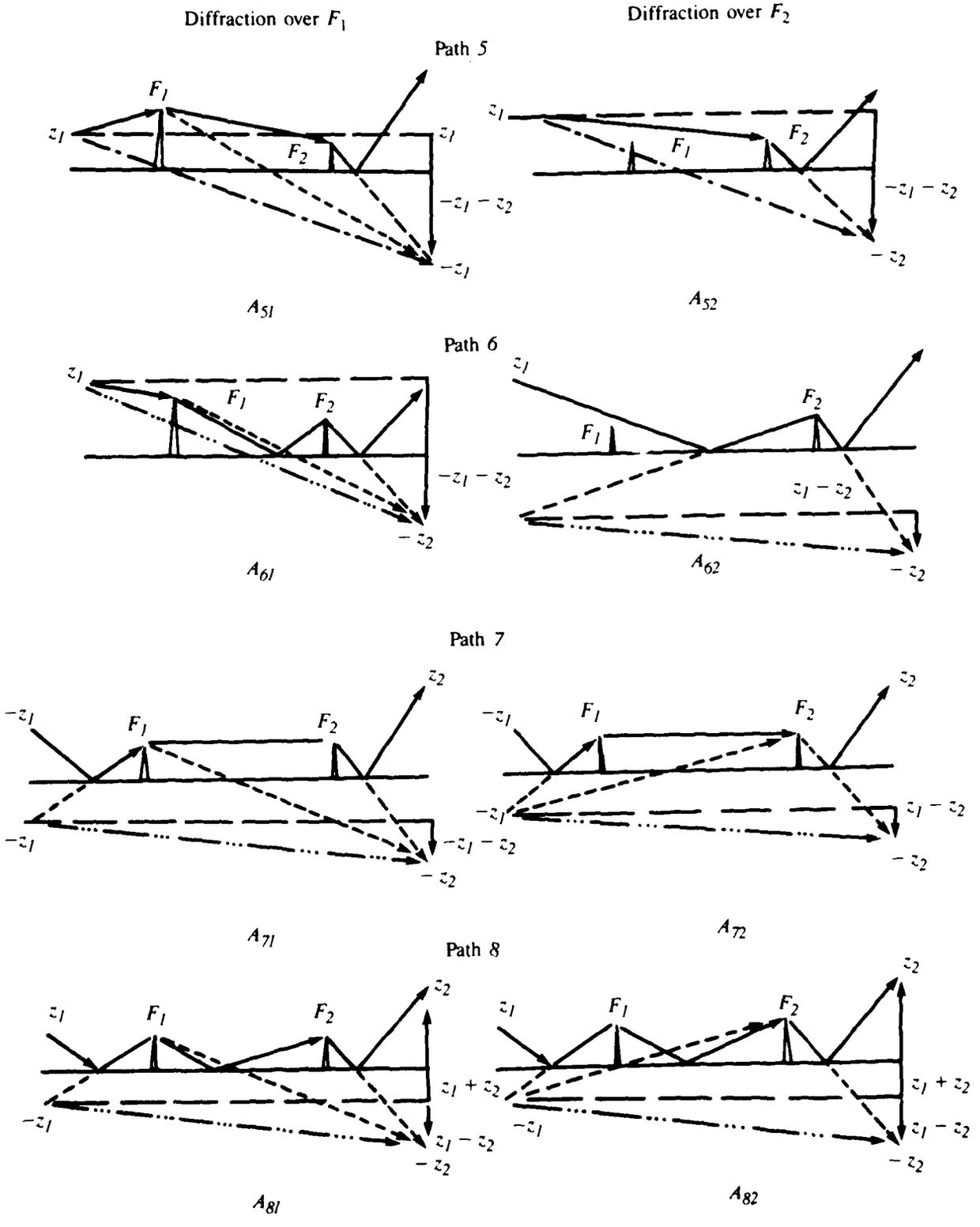

Figure A-1. Indirect ray paths and their corresponding normalized electric amplitudes (cont'd).

Appendix B. -- Computer Program DOUBLEDGE

Listed below are the input parameters of the computer program DOUBLEDGE:

*Geometric parameters**

Z1	is antenna height
Z2S	is minimal receiver height
Z2E	is maximal hypothetical receiver height of interest
DZ2	is step in meters to next height level of receiver
D1	is distance from transmitter to first knife edge
D2	is distance from first knife edge to second one
D3	is distance from second knife edge to receiver
F1	is height of first knife edge
F2	is height of second knife edge

Electric and terrain parameters

EPSLN1	is ε_1, which is the relative dielectric constant** over D1
EPSLN2	is ε_2, which is the relative dielectric constant* over D2
EPSLN3	is ε_3, which is the relative dielectric constant** over D3
S1	is conductivity of the ground† over D1 in mhos/meters
S2	is conductivity of the ground† over D2 in mhos/meters
S3	is conductivity of the ground† over D3 in mhos/meters
REFL1	is the roughness‡ factor over D1
REFL2	is the roughness‡ factor over D2
REFL3	is the roughness‡ factor over D3
RLAMDA	is the wavelength in meters
POLR	is the polarization of the electric field **E** and may be either horizontal "H" or vertical "V"

AEOLOTROPIC is a parameter that distinguishes between a beamed radar signal and a broadcast/isotropic lower frequency signal. It is therefore input as either "ANISOTROPIC" or as "ISOTROPIC," with an appropriate change in the wavelength RLAMDA

**All heights and distances are in meters.*

***This is also called permittivity.*

†The unit mho is a reciprocal ohm. One ohm is the same as one siemen in SI units.

‡This satisfies the Rayleigh criterion.

APPENDIX B

```
C       PROGRAM DOUBLEDGE

C       THIS MODEL CALCULATES THE PATTERN PROPAGATION FACTOR F FOR RADIO
C       PROPAGATION OVER FLAT TERRAIN ON WHICH 2 KNIFE-EDGE OBSTRUCTIONS
C       LIE PERPENDICULAR TO THE DIRECTION OF PROPAGATION.

C       INPUT:

C            GEOMETRICAL DISTANCES IN METERS
C            WAVELENGTH IN METERS
C            POLARIZATION: H OR V
C            GROUND PROPERTIES TO THE LEFT AND RIGHT OF EACH MASK

C       OUTPUT:

C            TABLE CONSISTING OF:
C               RADIATING SOURCE ANTENNA HEIGHT Z1 (IN METERS)
C               TARGET HEIGHT Z2 (METERS)
C               GRAZING ANGLES AT THE TRANSMITTER AND THE TARGET

C            VARIABLES THAT START WITH THE LETTER C ARE COMPLEX

      CHARACTER*1 POLAR(2), POLR
      CHARACTER*11 BEAM(2), AEOLOTROPIC
      COMPLEX CT1,CT2,CT3,CF,CTH,CTV
      COMPLEX CE11,CE12,CE21,CE31,CE41
      COMPLEX CE52,CE62,CE71,CE72,CE81,CE82
      COMPLEX CE32, CE42, CE22, CE51, CE61

      REAL*8 R1,R2,R3,R4,R5,R6,R7,R8,A,B,VTERM,DD,D
      REAL*8 VC11,VC12,VC21,VC31,VC41
      REAL*8 VC52,VC62,VC71,VC72,VC81,VC82
      REAL*8 VS11,VS12,VS21,VS31,VS41
      REAL*8 VS52,VS62,VS71,VS72,VS81,VS82
      REAL*8 VC32,VC42,VC22,VC51,VC61
      REAL*8 VS32,VS42,VS22,VS51,VS61
      REAL*4 RLAMDA

      DATA POLAR/'H','V'/
      DATA BEAM/'ANISOTROPIC','ISOTROPIC'/

C     OPEN INPUT AND OUTPUT FILES, AND DEFINE SOME QUANTITIES.
      OPEN(1, NAME = 'DOUBLEDGE.DAT', TYPE = 'OLD')
      OPEN(2, NAME = 'DOUBLEDGE.OUT', TYPE = 'NEW')

      READ(1,*) LCASES

      PI = 3.14159
      RAD = 57.29578
      SQRT2 = SQRT(2.0)

      AA = -82914.54
      BB = 126.3854
      CC = 48.07834
      RCS = 1.        ! RADAR CROSS-SECTION

      DO 300 ICASE = 1, LCASES
C     READ GEOMETRIC PARAMETERS.

C     THREE RECORDS CONSTITUTE A SUB-FILE
```

```
C       READ GEOMETRIC PARAMETERS

C       Z1    IS ANTENNA HEIGHT
C       Z2S   IS MINIMAL RECEIVER HEIGHT
C       Z2E   IS MAXIMAL HYPOTHETICAL RECEIVER HEIGHT OF INTEREST
C       DZ2   IS STEP IN METERS TO NEXT HEIGHT LEVEL OF RECEIVER
C       D1    IS DISTANCE FROM TRANSMITTER TO FIRST KNIFE EDGE
C       D2    IS DISTANCE FROM FIRST KNIFE EDGE TO THE SECOND ONE
C       D3    IS DISTANCE FROM THE SECOND KNIFE EDGE TO THE RECEIVER
C       F1    IS HEIGHT OF FIRST KNIFE EDGE
C       F2    IS HEIGHT OF SECOND KNIFE EDGE

        READ(1,*, END = 16) Z1, Z2S, Z2E, DZ2, D1, D2, D3, F1, F2

C       READ IN DIELECTRIC CONSTANTS AND FRESNEL FACTORS AND WAVELENGTH
C          EPSLN1 IS EPSILON (PERMITIVITY) - RELATIVE DIELECTRIC
C                    CONSTANT OVER D1
C          EPSLN2 IS EPSILON (PERMITIVITY) - RELATIVE DIELECTRIC
C                    CONSTANT OVER D2
C          EPSLN3 IS EPSILON (PERMITIVITY) - RELATIVE DIELECTRIC
C                    CONSTANT OVER D3
C          S1     IS CONDUCTIVITY OF GROUND OVER D1 IN MHOS/METER
C          S2     IS CONDUCTIVITY OF GROUND OVER D2 IN MHOS/METER
C          S3     IS CONDUCTIVITY OF GROUND OVER D3 IN MHOS/METER
C          REFL1  IS ROUGHNESS FACTOR OVER D1
C          REFL2  IS ROUGHNESS FACTOR OVER D2
C          REFL3  IS ROUGHNESS FACTOR OVER D3
C          RLAMDA IS WAVELENGTH IN METERS

        READ(1,*) EPSLN1, EPSLN2, EPSLN3, S1, S2, S3, REFL1,
     1            REFL2, REFL3, RLAMDA

C          POLR   IS POLARIZATION, AND MAY EITHER BE VERTICAL "V"
C                    OR HORIZONTAL "H".
C       READ IN POLARIZATION
        READ(1,3) POLR
C          ANISOTROPIC/AEOLOTROPIC MEANS THAT THE MICROWAVES ARE
C          BEAMED & THEREFORE NOT BROADCAST (I.E., IS ISOTROPIC)
        READ(1,4) AEOLOTROPIC

        IF(POLR.EQ.POLAR(1)) IPOL = 1
        IF(POLR.EQ.POLAR(2)) IPOL = 2

        IF(AEOLOTROPIC.EQ.BEAM(1)) ITROPIC = 1
        IF(AEOLOTROPIC.EQ.BEAM(2)) ITROPIC = 2

C       INITIALIZE SOME VALUES BEFORE THE MAIN PROCESSING LOOP: Z2 IS
C       THE HEIGHT OF RECEIVER (M), LAMDA IS THE WAVELENGTH.

        Z2 = Z2S -DZ2

C       ECHO CHECK THE INPUTS AND PREPARE THE OUTPUT TABLE.

        WRITE(2,10) Z1, D1, D2, D3, F1, F2, RLAMDA, POLR, EPSLN1,
     1              EPSLN2 ,EPSLN3, S1, S2, S3, REFL1, REFL2, REFL3

C       CALCULATE THE TWO CLEARANCE PARAMETERS

C       FIRST PARAMETER
        H01 = RLAMDA * D1 * D2
```

APPENDIX B

```
      HO2 = D1 +D2
      HOO1 = SQRT(HO1/HO2)

C     SECOND PARAMETER
      HO3  = RLAMDA * D2 * D3
      HO4  = D2 +D3
      HOO2 = SQRT(HO3/HO4)

C     MAIN PROCESSING LOOP: LOOP OVER TARGET HEIGHT FROM INITIAL
C     TARGET HEIGHT TO FINAL TARGET HEIGHT BY THE INCREMENT DZ2

  100 Z2 = Z2 +DZ2
      IF(Z2 .GT. Z2E) GOTO 1000

C     COMPUTE THE GRAZING ANGLES FOR CHANGES OF TARGET HEIGHT
      TTHETA2 = (Z1 +Z2)/(D1 +D2 +D3*1.0D+00)
      TTHETA1 = (Z2 -Z1)/(D1 +D2 +D3*1.0D+00)
      PHI     = TTHETA1 +TTHETA2

      IF(ITROPIC .EQ. 1) GO TO 102
      GRdB = 1.
      IF(ITROPIC .EQ. 2) GO TO 101
  102 CONTINUE
      G    = AA*PHI*PHI +BB*PHI +CC
      SUPER = (G -CC)/20.
      GRdB  = 10.**SUPER
C     CALCULATE R1, R2, R3, AND R4

  101 CONTINUE
      R1 = SQRT((Z2 -Z1)**2 +(D1 +D2 +D3)**2)
      R2 = SQRT((Z1 +Z2)**2 +(D1 +D2 +D3)**2)
      R3 = R2
      R4 = R1
      R5 = R2
      R6 = R1
      R7 = R1
      R8 = R1

C     CALCULATION OF DIFFRACTION CLEARANCE - DELTA PARAMETERS

C     CALCULATE V11, V12, V21, V31, V41,
C               V52, V62, V71, V72, V81, V82, V61,
C     ALSO CALCULATE V32, V42, V22, V42, V51 @ THE END OF THIS
C       GROUPING OF INSTRUCTIONS

      D  = D1 +D2*1.0D+00
      DD = D  +D3

C     CLEARANCE DELTA IS  (Z1 +VTERM -F1) & DELTA-ZERO IS HOO1
      VTERM = (Z2 -Z1)*D1/DD
      V11   = SQRT2 * (Z1 +VTERM -F1)/HOO1
      ! INTERPRETATION. DIRECT CASE.

C     CLEARANCE DELTA IS  (Z1 +VTERM -F2) & DELTA-ZERO IS HOO2
      VTERM = (Z2 -Z1)*D/DD
      V12   = SQRT2 * (Z1 +VTERM -F2)/HOO2
      ! INTERPRETATION. DIRECT CASE.

C     CLEARANCE DELTA IS (-Z1 +VTERM -F1) & DELTA-ZERO IS HOO1
      VTERM = (Z1 +Z2)*D1/DD
```

```
      V21    = SQRT2 * (-Z1 +VTERM -F1)/H001

C     CLEARANCE DELTA IS (Z1 +VTERM -F1) & DELTA-ZERO IS H001
      VTERM = (-Z1 -Z2)*D1/DD
      V31    = SQRT2 * (Z1 +VTERM -F1)/H001

C     CLEARANCE DELTA IS (-Z1 +VTERM -F1) & DELTA-ZERO IS H001
      VTERM = (Z1 -Z2)*D1/DD
      V41    = SQRT2 * (-Z1 +VTERM -F1)/H001

C     CLEARANCE DELTA IS  (Z1 +VTERM -F2) & DELTA-ZERO IS H002
      VTERM = (-Z1 -Z2)*D/DD
      V52    = SQRT2 * (Z1 +VTERM -F2)/H002

C     CLEARANCE DELTA IS (-Z1 +VTERM -F2) & DELTA-ZERO IS H002
      VTERM = (Z1 -Z2)*D/DD
      V62    = SQRT2 * (-Z1 +VTERM -F2)/H002

C     CLEARANCE DELTA IS (-Z1 +VTERM -F1) & DELTA-ZERO IS H001
      VTERM = (Z1 -Z2)*D1/DD
      V71    = SQRT2 * (-Z1 +VTERM -F1)/H001

C     CLEARANCE DELTA IS (-Z1 +VTERM -F2) & DELTA-ZERO IS H002
      VTERM = (Z1 -Z2)*D/DD
      V72    = SQRT2 * (-Z1 +VTERM -F2)/H002

C     CLEARANCE DELTA IS (-Z1 +VTERM -F1) & DELTA-ZERO IS H001
      VTERM = (-Z2 +Z1)*D1/DD
      V81    = SQRT2 * (-Z1 +VTERM -F1)/H001

C     CLEARANCE DELTA IS (-Z1 +VTERM -F2) & DELTA-ZERO IS H002
      VTERM = (-Z2 +Z1)*D/DD
      V82    = SQRT2 * (-Z1 +VTERM -F2)/H002

      VTERM = (Z1 +Z2)*D/DD
      V32    = SQRT2 * (-Z1 +VTERM -F2)/H002

      VTERM = (Z1 +Z2)*D/DD
      V42    = SQRT2 * (-Z1 +VTERM -F2)/H002

      VTERM = (Z1 +Z2)*D/DD
      V22    = SQRT2 * (-Z1 +VTERM -F2)/H002

      VTERM = (-Z1 -Z2)*D1/DD
      V51    = SQRT2 * (Z1 +VTERM -F1)/H001

      VTERM = (-Z1 -Z2)*D1/DD
      V61    = SQRT2 * (Z1 +VTERM -F1)/H001

C TEST FOR CHOICE OF DIRECT PATH PAY
            ALPHA1 = ATAN( (F1 -Z1)/D1 )
            ALPHA2 = ATAN( (F2 -Z1)/D )

C     IF( (F1. LT. F2) .AND. (ALPHA1 .LT. ALPHA2) ) THEN
C       GO TO 52
C     ELSE
C        GO TO 50
C     END IF

C     IF( (F1 .LT. F2) .AND. (ALPHA1 .GE. ALPHA2) ) THEN
```

APPENDIX B

```
C         GOTO 50
C      ELSE
C         GO TO 52
C      END IF

C      IF( (F1 .GE. F2) .AND. (ALPHA1 .GE. ALPHA2) ) THEN
C         GO TO 50
C      ELSE
C         GO TO 52
C      END IF

       IF( (F1 .LT. F2) .AND. (ALPHA1 .LT. ALPHA2) ) GOTO 52
       IF( (F1 .LT. F2) .AND. (ALPHA1 .GE. ALPHA2) ) GOTO 50
       IF( (F1 .LT. F2) .AND. (ALPHA1 .GE. ALPHA2) ) GOTO 50

C                 CALCULATE A11 USING V11 CORRESP. TO F1

   50              CALL DCS(VC11, VS11, V11)
                   A11 = 1./SQRT2 * DSQRT((VC11 +0.5)**2 +(VS11 +0.5)**2)

                   IF(VC11 +0.5 .GE. 0.) THEN
                      B = DATAN( (VS11 +0.5)/(VC11 +0.5) ) -PI/4.
                   ELSE
                      B = PI +DATAN( (VS11 +0.5)/(VC11 +0.5) ) -PI/4.
                   END IF
                   A1 = A11 * DSIN(B)
                   B1 = A11 * DCOS(B)
                   CE11 = CMPLX(B1,A1)
                   CE1  = CE11
                   GOTO 53

C                  CALCULATE A12 USING V12 CORRESP. TO F2

   52              CALL DCS(VC12, VS12, V12)
                   A12 = 1./SQRT2 * DSQRT((VC12 +0.5)**2 +(VS12 +0.5)**2)

                   IF(VC12 +0.5 .GE. 0.) THEN
                      B = DATAN((VS12 +0.5)/(VC12 +0.5)) -PI/4.
                   ELSE
                      B = PI +DATAN((VS12 +0.5)/(VC12 +0.5)) -PI/4.
                   END IF

                   A1 = A12 * DSIN(B)
                   B1 = A12 * DCOS(B)
                   CE12 = CMPLX(B1,A1)
                   CE1  = CE12

C        COMPUTATION OF GRAZING ANGLE PSI1 OVER D1,
C        PSI2 OVER D2, AND PSI3 OVER D3.

C        GRAZING ANGLE FOR PATH 21
    53   IF(V21 .GE. 0.) GOTO 200

C        RAY INTERSECTS THE MASK F1
         PSI1 = DATAN( (Z1 +F1)/D1*1.0D+00)
         GOTO 201

C        RAY IS CLEAR OF THE MASK F1
   200   CONTINUE
         PSI1 = DATAN( (Z2 +Z1)/DD)
```

```
  201   CONTINUE

C       CALL THE COMPLEX REFLECTION SUBROUTINE FOR THE
C       TERRAIN REGION D1
        CALL FRESNL(EPSLN1,RLAMDA,S1,PSI1,CTH,CTV)

C       MULTIPLY BY FACTORS
        CTH = CTH * REFL1
        CTV = CTV * REFL1

C       SET CT1 OVER D1
        IF(IPOL .EQ. 1) CT1 = CTH
        IF(IPOL. EQ. 2) CT1 = CTV

C       888 SHOWS NO REFLECTION OVER D1
        IF(EPSLN1 .EQ. 888. .AND. S1 .EQ. 888.) CT1 = CMPLX(0.0,0.0)

C       CALCULATE A21 USING V21 CORRESP. TO F1

        CALL DCS(VC21, VS21, V21)
        A21 = 1./SQRT2 * DSQRT((VC21 +0.5)**2 +(VS21 +0.5)**2)

C       GRAZING ANGLE FOR PATH 22
        IF(V22 .GE. 0.) GOTO 220

C       RAY INTERSECTS THE MASK F2
        PSI1 = DATAN( (Z1 +F2)/D)
        GOTO 221

C       RAY IS CLEAR OF THE MASK F2
  220   CONTINUE
        PSI1 = DATAN( (Z1 +Z2)/DD)

  221   CONTINUE

        CALL FRESNL(EPSLN1,RLAMDA,S1,PSI1,CTH,CTV)
        CTH = CTH * REFL1
        CTV = CTV * REFL1
        IF(IPOL .EQ. 1) CT1 = CTH
        IF(IPOL .EQ. 2) CT1 = CTV
        IF(EPSLN1 .EQ. 888. .AND. S1 .EQ. 888.) CT1 = CMPLX(0.0,0.0)

C       CALCULATE CF22 USING V22 CORRESP. TO F2

        CALL DCS(VC22, VS22, V22)
        A22 = 1./SQRT2 * DSQRT((VC22 +0.5)**2 +(VS22 +0.5)**2)

        IF(VC22 +0.5 .GE. 0.) THEN
           B = DATAN((VS22 +0.5)/(VC22 +0.5)) -PI/4.
        ELSE
           B = PI +DATAN((VS22 +0.5)/(VC22 +0.5)) -PI/4.
        END IF
        A1 = A22 * A21 * DSIN(B)
        B1 = A22 * A21 * DCOS(B)
        CF22 = CMPLX(B1,A1) * CT1 * GRdB

C               GRAZING ANGLE FOR PATH 31
                IF(V31 .GE. 0.) GOTO 310
```

APPENDIX B

```
C                RAY INTERSECTS THE MASK F1
                 PSI1 = DATAN( (Z2 +F1)/(D2 +D3*1.0D+00) )
                 GOTO 301

C                RAY IS CLEAR OF THE MASK F1
  310            CONTINUE
                 PSI1 = DATAN( (Z1 +Z2)/DD)

  301            CONTINUE

           CALL FRESNL(EPSLN1, RLAMDA,S1,PSI1,CTH,CTV)
           CTH = CTH * REFL1
           CTV = CTV * REFL1
           IF(IPOL .EQ. 1) CT1 = CTH
           IF(IPOL .EQ. 2) CT1 = CTV
           IF(EPSLN1 .EQ. 888. .AND. S1 .EQ. 888.) CT1 = CMPLX(0.0,0.0)

C                CALCULATE A31 USING V31 CORRESP. TO F1

                 CALL DCS(VC31, VS31, V31)
                 A31 = 1./SQRT2 * DSQRT((VC31 +0.5)**2 +(VS31 +0.5)**2)

C                GRAZING ANGLE FOR PATH 32
                 IF(V32 .GE. 0.) GOTO 320

C                RAY INTERSECTS THE MASK F2
                 PSI1 = DATAN( (Z1 +F2)/D)
                 GOTO 321

C                RAY IS CLEAR OF THE MASK F2
  320            CONTINUE
                 PSI1 = DATAN( (Z1 +Z2)/DD)

  321            CONTINUE

           CALL FRESNL(EPSLN1,RLAMDA,S1,PSI1,CTH,CTV)
           CTH = CTH * REFL1
           CTV = CTV * REFL1
           IF(IPOL .EQ. 1) CT1 = CTH
           IF(IPOL. EQ. 2) CT1 = CTV
           IF(EPSLN1 .EQ. 888. .AND. S1 .EQ. 888.) CT1 = CMPLX(0.0,0.0)

C                CALCULATE CE32 USING V32 CORRESP. TO F2

                 CALL DCS(VC32, VS32, V32)
                 A32 = 1./SQRT2 * DSQRT((VC32 +0.5)**2 +(VS32 +0.5)**2)

                 IF(VC32 +0.5 .GE. 0.) THEN
                    B = DATAN((VS32 +0.5)/(VC32 +0.5)) -PI/4.
                 ELSE
                    B = PI +DATAN((VS32 +0.5)/(VC32 +0.5)) -PI/4.
                 END IF
                 A1 = A32 * A31 * DSIN(B)
                 B1 = A32 * A31 * DCOS(B)
                 CE32 = CMPLX(B1,A1) * CT2 * GRdB

C          GRAZING ANGLE FOR PATH 41
           IF(V41 .GE. 0. ) GOTO 400

C          RAY INTERSECTS THE MASK F1
```

```
      PSI1 = DATAN(  (F1 +Z1)/ D1 * 1.0D+00  )
      PSI2 = DATAN(  (Z2 +F1)/ D  )

        CALL FRESNL(EPSLN1,RLAMDA,S1,PSI1,CTH,CTV)
        CTH = CTH * REFL1
        CTV = CTV * REFL1
        IF(IPOL .EQ. 1) CT1 = CTH
        IF(IPOL .EQ. 2) CT1 = CTV
        IF(EPSLN1 .EQ. 888. .AND. S1 .EQ. 888.) CT1 = CMPLX(0.0,0.0)

C       CALL THE COMPLEX COEFFICIENT OVER D2
        CALL FRESNL(EPSLN2,RLAMDA,S2,PSI2,CTH,CTV)

C       MULTIPLY BY FACTORS
        CTH = CTH * REFL2
        CTV = CTV * REFL2

C       SET CT2 OVER D2
        IF(IPOL .EQ. 1) CT2 = CTH
        IF(IPOL .EQ. 2) CT2 = CTV

C       888 SHOWS 0 REFLECTION OVER D2
        IF(EPSLN2 .EQ. 888. .AND. S2 .EQ. 888.) CT2 = CMPLX(0.0,0.0)

      GOTO 401

C     RAY IS CLEAR OF THE MASK F1
  400 CONTINUE
      PSI1 = DATAN( (Z1 -Z2)/ DD )

        CALL FRESNL(EPSLN1,RLAMDA,S1,PSI1,CTH,CTV)
        CTH = CTH * REFL1
        CTV = CTV * REFL1
        IF(IPOL .EQ. 1) CT1 = CTH
        IF(IPOL .EQ. 2) CT1 = CTV
        IF(EPSLN1 .EQ. 888. .AND. S1 .EQ. 888.) CT1 = CMPLX(0.0,0.0)

  401 CONTINUE

C     CALCULATE A41 USING V41 CORRESP. TO F1

      CALL DCS(VC41, VS41, V41)
      A41 = 1./SQRT2 * DSQRT((VC41 + 0.5)**2 + (VS41 + 0.5)**2)

C     GRAZING ANGLE FOR PATH 42
      IF(V42 .GE. 0. ) GOTO 420

C     RAY INTERSECTS THE MASK F2
      PSI1 = DATAN( (Z1 +F1) / D1 * 1.0D+00 )
C     PSI2 = DATAN( (Z1 +F2)/D)

         CALL FRESNL(EPSLN1,RLAMDA,S1,PSI1,CTH,CTV)
         CTH = CTH * REFL1
         CTV = CTV * REFL1
         IF(IPOL .EQ. 1) CT1 = CTH
         IF(IPOL .EQ. 2) CT1 = CTV
         IF(EPSLN1 .EQ. 888. .AND. S1 .EQ. 888.) CT1 = CMPLX(0.0,0.0)

         CALL FRESNL(EPSLN2,RLAMDA,S2,PSI2,CTH,CTV)
         CTH = CTH * REFL2
```

```
            CTV = CTV * REFL2
            IF(IPOL .EQ. 1) CT2 = CTH
            IF(IPOL .EQ. 2) CT2 = CTV
            IF(EPSLN2 .EQ. 888. .AND. S2 .EQ. 888.) CT2 = CMPLX(0.0,0.0)
          GOTO 421

C         RAY IS CLEAR OF THE MASK F2
  420     CONTINUE
          PSI1 = DATAN( (Z1 +Z2)/DD)

            CALL FRESNL(EPSLN1,RLAMDA,S1,PSI1,CTH,CTV)
            CTH = CTH * REFL1
            CTV = CTV * REFL1
            IF(IPOL .EQ. 1) CT1 = CTH
            IF(IPOL .EQ. 2) CT1 = CTV
            IF(EPSLN1 .EQ. 888. .AND. S1 .EQ. 888.) CT1 = CMPLX(0.0,0.0)
  '
   421    CONTINUE

C         CALCULATE CE42 USING V42 CORRESP. TO F2

          CALL DCS(VC42, VS42, V42)
          A42 = 1./SQRT2 * DSQRT((VC42 +0.5)**2 +(VS42 +0.5)**2)

          IF(VC42 +0.5 .GE. 0.) THEN
             B = DATAN((VS42 +0.5)/(VC42 +0.5)) -PI/4.
          ELSE
             B = PI +DATAN((VS42 +0.5)/(VC42 +0.5)) -PI/4.
          END IF
          A1 = A42 * A41 * DSIN(B)
          B1 = A42 * A41 * DCOS(B)
          CE42 = CMPLX(B1,A1) * CT1 * CT2 * GRdB

C                 GRAZING ANGLE FOR PATH 51
                  IF(V51 .GE. 0. ) GOTO 590

C                 RAY INTERSECTS THE MASK F1
                  PSI3 = DATAN( (Z2 +F2)/ D3*1.0D+00)

C               CALL THE COMPLEX COEFFICIENT OVER D3
                CALL FRESNL(EPSLN3,RLAMDA,S3,PSI3,CTH,CTV)

C               MULTIPLY BY FACTORS
                CTH = CTH * REFL3
                CTV = CTV * REFL3

C               SET CT3 OVER D3
                IF(IPOL .EQ. 1) CT3 = CTH
                IF(IPOL .EQ. 2) CT3 = CTV

C               IF(EPSLN3 .EQ. 888. .AND. S3 .EQ. 888.) CT3 = CMPLX(0.0,0.0)

                      GOTO 501

C                     RAY CLEAR OF THE MASK F1
  590                 CONTINUE
                      PSI1 = DATAN( (Z1 +Z2)/ DD)

                CALL FRESNL(EPSLN1,RLAMDA,S1,PSI1,CTH,CTV)
                CTH = CTH * REFL1
```

```
            CTV = CTV * REFL1
            IF(IPOL .EQ. 1) CT1 = CTH
            IF(IPOL .EQ. 2) CT1 = CTV
            IF(EPSLN1 .EQ. 888. .AND. S1 .EQ. 888.) CT1 = CMPLX(0.0,0.0)
  501             CONTINUE

C                 CALCULATE A51 USING V51 CORRESP. TO F1
                  CALL DCS(VC51, VS51, V51)
                  A51 = 1./SQRT2 * DSQRT((VC51 +0.5)**2 +(VS51 +0.5)**2)

C                 GRAZING ANGLE FOR PATH 52
                  IF(V52 .GE. 0. ) GOTO 520

C                 RAY INTERSECTS THE MASK F2
                  PSI3 = DATAN( (Z2 +F2)/D3 * 1.0D+00 )
            CALL FRESNL(EPSLN3,RLAMDA,S3,PSI3,CTH,CTV)
            CTH = CTH * REFL3
            CTV = CTV * REFL3
            IF(IPOL .EQ. 1) CT3 = CTH
            IF(IPOL .EQ. 2) CT3 = CTV
            IF(EPSLN3 .EQ. 888. .AND. S3 .EQ. 888.) CT3 = CMPLX(0.0,0.0)
                  GOTO 521

C                 RAY IS CLEAR OF THE MASK F2
  520             CONTINUE
                  PSI1 = DATAN( (Z1 +Z2)/ DD )
            CALL FRESNL(EPSLN1,RLAMDA,S1,PSI1,CTH,CTV)
            CTH = CTH * REFL1
            CTV = CTV * REFL1
            IF(IPOL .EQ. 1) CT1 = CTH
            IF(IPOL .EQ. 2) CT1 = CTV
            IF(EPSLN1 .EQ. 888. .AND. S1 .EQ. 888.) CT1 = CMPLX(0.0,0.0)
  521             CONTINUE

C                 CALCULATE CE52 USING V52 CORRESP. TO F2
C                 NOTE. DITTO AS ABOVE FOR CASE 51. R5 -R1 = 0
                  CALL DCS(VC52, VS52, V52)
                  A52 = 1./SQRT2 * DSQRT((VC52 +0.5)**2 +(VS52 +0.5)**2)

                  IF(VC52 + 0.5 .GE. 0.) THEN
                     B = DATAN((VS52 +0.5)/(VC52 +0.5)) -PI/4.
                  ELSE
                     B = PI +DATAN((VS52 +0.5)/(VC52 +0.5)) -PI/4.
                  END IF
                  B = B +(2. * PI)/ RLAMDA * (R5 -R1)
                  A1 = A51 * A52 * DSIN(B)
                  B1 = A52 * A51 * DCOS(B)
                  CE52 = CMPLX(B1,A1) * CT3 * GRdB

C  511  GRAZING ANGLE FOR PATH 61
       IF( V61 .GE. 0. ) GOTO 6000

C      RAY INTERSECTS THE MASK F1
       PSI2 = DATAN( (Z2 +F1) / (D2 +D3*1.0D+00 ) )
       PSI3 = DATAN( (Z2 +F2) / D3 * 1.0D+00 )

          CALL FRESNL(EPSLN2,RLAMDA,S2,PSI2,CTH,CTV)
          CTH = CTH * REFL2
          CTV = CTV * REFL2
          IF(IPOL .EQ. 1) CT2 = CTH
```

```
            IF(IPOL .EQ. 2) CT2 = CTV
            IF(EPSLN2 .EQ. 888. .AND. S2 .EQ. 888.) CT2 = CMPLX(0.0,0.0)

            CALL FRESNL(EPSLN3,RLAMDA,S3,PSI3,CTH,CTV)
            CTH = CTH * REFL3
            CTV = CTV * REFL3
            IF(IPOL .EQ. 1) CT3 = CTH
            IF(IPOL .EQ. 2) CT3 = CTV
            IF(EPSLN3 .EQ. 888. .AND. S3 .EQ. 888.) CT3 = CMPLX(0.0,0.0)
          GOTO 601

C         RAY CLEAR OF THE MASK F1
 6000     CONTINUE
          PSI1 = DATAN( (Z1 +Z2)/DD )

            CALL FRESNL(EPSLN1,RLAMDA,S1,PSI1,CTH,CTV)
            CTH = CTH * REFL1
            CTV = CTV * REFL1
            IF(IPOL .EQ. 1) CT1 = CTH
            IF(IPOL .EQ. 2) CT1 = CTV
            IF(EPSLN1 .EQ. 888. .AND. S1 .EQ. 888.) CT1 = CMPLX(0.0,0.0)
   601    CONTINUE

C         CALCULATE A61 USING V61 CORRESP. TO F1

          CALL DCS(VC61, VS61, V61)
          A61 = 1./SQRT2 * DSQRT((VC61 +0.5)**2 +(VS61 +0.5)**2)

C         GRAZING ANGLE FOR PATH 62
          IF(V62 .GE. 0. ) GOTO 620

C         RAY INTERSECTS THE MASK F2
          PSI2 = DATAN( (Z1 + F2) / D )
          PSI3 = DATAN( (F2 +Z2)/D3 * 1.0D+00 )
             CALL FRESNL(EPSLN2,RLAMDA,S2,PSI2,CTH,CTV)
             CTH = CTH * REFL2
             CTV = CTV * REFL2
             IF(IPOL .EQ. 1) CT2 = CTH
             IF(IPOL .EQ. 2) CT2 = CTV
             IF(EPSLN2 .EQ. 888. .AND. S2 .EQ. 888.) CT2 = CMPLX(0.0,0.0)

             CALL FRESNL(EPSLN3,RLAMDA,S3,PSI3,CTH,CTV)
             CTH = CTH * REFL3
             CTV = CTV * REFL3
             IF(IPOL .EQ.1 ) CT3 = CTH
             IF(IPOL .EQ. 2) CT3 = CTV
             IF(EPSLN3 .EQ. 888. .AND. S3 .EQ. 888.) CT3 = CMPLX(0.0,0.0)
          GOTO 621

C         RAY CLEAR OF THE MASK F2
   620    CONTINUE
          PSI1 = DATAN( (Z1 -Z2)/ DD )

             CALL FRESNL(EPSLN1,RLAMDA,S1,PSI1,CTH,CTV)
             CTH = CTH * REFL1
             CTV = CTV * REFL1
             IF(IPOL .EQ. 1) CT1 = CTH
             IF(IPOL .EQ. 2) CT1 = CTV
             IF(EPSLN1 .EQ. 888. .AND. S1 .EQ. 888.) CT1 = CMPLX(0.0,0.0)
   621    CONTINUE
```

```
C       CALCULATE CE62 USING V62 CORRESP. TO F2
C       NOTE. DITTO AS ABOVE FOR CASE 52. R6 -R1 = 0
        CALL DCS(VC62, VS62, V62)
        A62 = 1./SQRT2 * DSQRT((VC62 +0.5)**2 +(VS62 +0.5)**2)

        IF(VC62 +0.5 .GE. 0.) THEN
           B = DATAN((VS62 +0.5)/(VC62 +0.5)) -PI/4.
        ELSE
           B = PI +DATAN((VS62 +0.5)/(VC62 +0.5)) -PI/4.
        END IF

        A1 = A61 * A62 * DSIN(B)
        B1 = A62 * A61 * DCOS(B)
        CE62 = CMPLX(B1,A1) * CT2 * CT3 * GRdB

C               GRAZING ANGLE FOR PATH 71
                IF (V71 .GE. 0.) GOTO 7000

C               RAY INTERSECTS THE MASK F1
                PSI1 = DATAN( (F1 +Z1)/D1 * 1.0D+00 )
                GOTO 701

C               RAY CLEAR OF THE MASK F1
 7000           CONTINUE
                PSI1 = DATAN( (Z1 -Z2)/ DD )
  701           CONTINUE
            CALL FRESNL(EPSLN1,RLAMDA,S1,PSI1,CTH,CTV)
            CTH = CTH * REFL1
            CTV = CTV * REFL1
            IF(IPOL .EQ. 1) CT1 = CTH
            IF(IPOL .EQ. 2) CT1 = CTV
            IF(EPSLN1 .EQ. 888. .AND. S1 .EQ. 888.) CT1 = CMPLX(0.0,0.0)

C               CALCULATE A71 USING V71 CORRESP. TO F1
C               NOTE. DITTO AS ABOVE FOR CASE 51.  R7 -R1 = 0
                CALL DCS(VC71,VS71,V71)
                A71 = 1./SQRT2 * DSQRT((VC71 +0.5)**2 +(VS71 +0.5)**2)

C               GRAZING ANGLE FOR PATH 72
                IF(V72 .GE. 0.) GOTO 720

C               RAY INTERSECTS THE MASK F2
                PSI3 = DATAN( (Z2 +F2) / D3 * 1.0D+00 )
            CALL FRESNL(EPSLN3,RLAMDA,S3,PSI3,CTH,CTV)
            CTH = CTH * REFL3
            CTV = CTV * REFL3
            IF(IPOL .EQ. 1) CT3 = CTH
            IF(IPOL .EQ. 2) CT3 = CTV
            IF(EPSLN3 .EQ. 888. .AND. S3 .EQ. 888.) CT3 = CMPLX(0.0,0.0)
                GOTO 721

C               RAY CLEAR OF THE MASK F2
  720           CONTINUE
                PSI1 = DATAN( (Z1 -Z2)/DD )
            CALL FRESNL(EPSLN1,RLAMDA,S1,PSI1,CTH,CTV)
            CTH = CTH * REFL1
            CTV = CTV * REFL1
            IF(IPOL .EQ. 1) CT1 = CTH
            IF(IPOL .EQ. 2) CT1 = CTV
```

```
            IF(EPSLN1 .EQ. 888. .AND. S1 .EQ. 888.) CT1 = CMPLX(0.0,0.0)
  721       CONTINUE

C             CALCULATE CE72 USING V72 CORRESP. TO F2
C             NOTE.  DITTO AS ABOVE FOR CASE 51.  R7 -R1 = 0
              CALL DCS(VC72, VS72, V72)
              A72 = 1./SQRT2 * DSQRT((VC72 +0.5)**2 +(VS72 +0.5)**2)

              IF(VC72 +0.5 .GE. 0.) THEN
                 B = DATAN((VS72 +0.5)/(VC72 +0.5)) -PI/4.
              ELSE
                 B = PI +DATAN((VS72 +0.5)/(VC72 +0.5)) -PI/4.
              END IF

              A1 = A72 * A71 * DSIN(B)
              B1 = A72 * A71 * DCOS(B)
              CE72 = CMPLX(B1,A1) * CT1 * CT3 * GRdB

C       GRAZING ANGLE FOR PATH 81
        IF(V81 .GE. 0.) GOTO 800

C       RAY INTERSECTS THE MASK F1
        PSI1 = DATAN( ( Z1 +F1)/D1 * 1.0D+00 )
        PSI2 = DATAN( (F1 +Z2)/(D2 +D3 * 1.0D+00 ) )

           CALL FRESNL(EPSLN1,RLAMDA,S1,PSI1,CTH,CTV)
           CTH = CTH * REFL1
           CTV = CTV * REFL1
           IF(IPOL .EQ. 1) CT1 = CTH
           IF(IPOL .EQ. 2) CT1 = CTV
           IF(EPSLN1 .EQ. 888. .AND. S1 .EQ. 888.) CT1 = CMPLX(0.0,0.0)

           CALL FRESNL(EPSLN2,RLAMDA,S2,PSI2,CTH,CTV)
           CTH = CTH * REFL2
           CTV = CTV * REFL2
           IF(IPOL .EQ. 1) CT2 = CTH
           IF(IPOL .EQ. 2) CT2 = CTV
           IF(EPSLN2 .EQ. 888. .AND. S2 .EQ. 888.) CT2 = CMPLX(0.0,0.0)
        GOTO 801

C       RAY CLEAR OF THE MASK F1
  800   CONTINUE
        PSI1 = DATAN( (F2 +Z2)/D3 * 1.0D+00 )
  801   CONTINUE

C       CALCULATE A81 USING V81 CORRESP. TO F1

        CALL DCS(VC81, VS81, V81)
        A81 = 1./SQRT2 * DSQRT((VC81 +0.5)**2 +(VS81 +0.5)**2)

C       GRAZING ANGLE FOR PATH 82
        IF(V82 .GE. 0.)  GOTO 820

C       RAY INTERSECTS THE MASK F2
        PSI3 = DATAN( (F2 +Z2)/ D3 * 1.0D+00 )

           CALL FRESNL(EPSLN3,RLAMDA,S3,PSI3,CTH,CTV)
           CTH = CTH * REFL3
           CTV = CTV * REFL3
           IF(IPOL .EQ. 1) CT3 = CTH
```

```
            IF(IPOL .EQ. 2) CT3 = CTV
            IF(EPSLN3 .EQ. 888. .AND. S3 .EQ. 888.) CT3 = CMPLX(0.0,0.0)
          GOTO 821

C         RAY IS CLEAR OF THE MASK F2
  820     CONTINUE
          PSI1 = DATAN( (Z1 -Z2)/ DD )

            CALL FRESNL(EPSLN1,RLAMDA,S1,PSI,CTH,CTV)
            CTH = CTH * REFL1
            CTV = CTV * REFL1
            IF(IPOL .EQ.1) CT1 = CTH
            IF(IPOL .EQ.2) CT1 = CTV
            IF(EPSLN1 .EQ. 888. .AND. S1 .EQ. 888.) CT1 = CMPLX(0.0,0.0)
  821     CONTINUE

C         CALCULATE CE82 USING V82 CORRESP. TO F2

          CALL DCS(VC82, VS82, V82)
           A82 = 1./SQRT2 * DSQRT((VC82 +0.5)**2 +(VS82 +0.5)**2)

            IF(VC82 +0.5 .GE. 0.) THEN
                B = DATAN((VS82 +0.5)/(VC82 +0.5)) -PI/4.
              ELSE
                  B = PI +DATAN((VS82 +0.5)/(VC82 +0.5)) -PI/4.
              END IF
               A1 = A82 * A81 * DSIN(B)
                B1 = A82 * A81 * DCOS(B)
                 CE82 = CMPLX(B1,A1) * CT1 * CT2 * CT3 * GRdB

C         CALCULATE COMPLEX F (CF)
C         BY FIRST CALCULATING THE COMPLEX PARTS CE11, CE12,
C         CE21, CE31, CE41, CE52, CE62, CE71, CE72, CE81, CE82
C         CE32, CE42, CE22, CE51, CE61

C         NOW ADD TO GET CF

          CF = +CE1 +CE22 +CE32 +CE42 +CE52 +CE62 +CE72 +CE82

          GOTO 216
C 215     CF = CE11 +CE21 +CE31 +CE41
C         WRITE OUT ANSWERS

  216     FO = CABS(CF)
          FLOG = 20. * ALOG10(FO)
          WRITE(2,*)
          WRITE(2,*)
          WRITE(2,11)
          WRITE(2,12)
          WRITE(2,14) FLOG, Z2
  700     WRITE(2,19)
          WRITE(2,20)
          WRITE(2,37)
          WRITE(2,18) V11, V21, V31, V41
          WRITE(2,38)
          WRITE(2,18) V12, V22, V32, V42
          WRITE(2,40)
          WRITE(2,18) V51, V52, V61, V62
          WRITE(2,46)
          WRITE(2,18) V71, V72, V81, V82
```

APPENDIX B

```
      GO TO 100

C     COME HERE WHEN FINISHED.

 1000 CONTINUE
      WRITE(2,600)  Z2S, Z2, DZ2
      WRITE(2,20)
  300 CONTINUE
   16 CLOSE(1)
      CLOSE(2)
      STOP
    1 FORMAT(' INPUT Z1, D1, D2, D3, F1, F2, Z2S, DZ2'/)
    2 FORMAT(' INPUT POLARIZATION.. H=HORIZONTAL,V=VERTICAL'/)
    3 FORMAT(A1)
    4 FORMAT(11A1)
   10 FORMAT(' ANTENNA HEIGHT (M):                          ' F6.2/
     1       ' DIST. FROM TRANSMITTER TO EDGE F1 (M): ',F10.1/
     2       ' DIST. FROM F1 TO EDGE F2 (M):          ',F10.1/
     3       ' DIST. FROM F2 TO TARGET RECEIVER (M):  ',F10.1/
     4       ' HEIGHT OF KNIFE EDGE F1 (M):           ',F10.1/
     5       ' HEIGHT OF KNIFE EDGE F2 (M):           ',F10.1/
     6       ' WAVELENGTH (M):                        ',F10.5/
     7       ' POLARIZATION:                          ',A1/
     8       ' EPSILON 1 (EPSLN1) OVER D1:            ',F8.3/
     9       ' EPSILON 2 (EPSLN2) OVER D2:            ',F8.3/
     1       ' EPSILON 3 (EPSLN3) OVER D3:            ',F8.3/
     2       ' SIGMA 1   (S1)     OVER D1:            ',F10.3/
     3       ' SIGMA 2   (S2)     OVER D2:            ',F10.3/
     4       ' SIGMA 3   (S3)     OVER D3:            ',F10.3/
     5       ' REFLECTION (REFL1) OVER D1:            ',F10.3/
     6       ' REFLECTION (REFL2) OVER D2:            ',F10.3/
     7       ' REFLECTION (REFL3) OVER D3:            ',F10.3//)
  600 FORMAT(' TARGET HT (M) FROM ',F5.0,' TO ',F8.4,' BY ',F5.1/)
   11 FORMAT(55H POWER GAIN IN    TARGET HT     POWER GAIN OF SCATTERED)
   12 FORMAT(55H db, 20 x LOG(F)  (METERS)     FIELD @ GROUND ZERO (db))
   14 FORMAT(3F15.4//)
   15 FORMAT(55HMAGNITUDES OF ELECTRIC FIELD COMPONENTS ASSOCIATED WITH)
   61 FORMAT(41H EACH RAY PATH, EXPRESSED IN VOLTS/METER/)
   17 FORMAT(55H   E11MAG       E21MAG         E31MAG         E41MAG    )
   18 FORMAT(4F15.4//)
   19 FORMAT(55H   INTEGRATION PARAM. OF FRESNEL INTEGRALS DERIVED FROM)
   20 FORMAT(25H   Z1, Z2, D1, D2, AND D3/)
   22 FORMAT(55H   GRAZING ANGLE      GRAZING ANGLE      GAIN REDUCTION)
   23 FORMAT(47H   AT SOURCE (RAD)    AT TARGET (RAD)    FACTOR/)
   25 FORMAT(39H   FRESNEL REFLECTION COEFFICIENT OVER:)
   26 FORMAT(46H          D1              D2                 D3/)
   28 FORMAT(35H   PHASE LAG ANGLE IN DEGREES OVER:)
   29 FORMAT(2F15.4//)
   30 FORMAT(51H   E12MAG         E22MAG         E32MAG         E42MAG)
   32 FORMAT(51H   E51MAG         E52MAG         E61MAG         E62MAG)
   33 FORMAT(27H          D1              D2/)
   34 FORMAT(54H                                        OFF-AXIS BEAM ANGLE)
   35 FORMAT(49H   TTHETA1 (RAD)   TTHETA2 (RAD)   OF ANTENNA PHI)
   37 FORMAT(49H       V11            V21            V31            V41)
   38 FORMAT(49H       V12            V22            V32            V42)
   40 FORMAT(49H       V51            V52            V61            V62)
   41 FORMAT(3F15.4////////)
   42 FORMAT(39H GRAZE ANGLE   GRAZE ANGLE  GRAZE ANGLE)
   43 FORMAT(55H AT SOURCE     OVER D2      OVER D3      GAIN REDUCTION)
```

```
   44 FORMAT(48H -RADIANS-      -RADIANS-     -RADIANS-     FACTOR/)
   45 FORMAT(51H   E71MAG         E72MAG        E81MAG        E82MAG)
   46 FORMAT(49H       V71            V72           V81           V82)
   47 FORMAT(8H   E1MAG)
   48 FORMAT(F15.4//)
      END

C ***************************************************************************

C      SUBROUTINE FOR COMPLEX REFLECTION COEFFICIENTS

       SUBROUTINE FRESNL(E1, WAVE, CONDUC, ANG, CTH, CTV)
       COMPLEX CAK, CTV, CTV1, CTV2, CTH, CTH1, CTH2

C      E1 ........... THE DIELECTRIC CONSTANT (FROM 0 TO 100)
C      LAMDA ........ THE WAVELENGTH IN METERS
C      CONDUC ....... THE CONDUCTIVITY IN MHOS/METER
C      ANG .......... THE ANGLE IN RADIANS

C      CALCULATE THE COMPLEX CONSTANT

       AKI = -60. * WAVE * CONDUC
       CAK = CMPLX(E1, AKI)

C      CALCULATE THE VERTICAL POLARIZATION REFLECTION COEFFICIENT

       CTV1 = CAK * SIN(ANG) -CSQRT(CAK -COS(ANG)**2)
       CTV2 = CAL * SIN(ANG) +CSQRT(CAK -COS(ANG)**2)
       CTV  = CTV1 / CTV2

C      CALCULATE THE HORIZONTAL POLARIZATION REFLECTION COEFFICIENT

       CTH1 = SIN(ANG) -CSQRT(CAK -COS(ANG)**2)
       CTH2 = SIN(ANG) +CSQRT(CAK -COS(ANG)**2)
       CTH  = CTH1 / CTH2

  1000 RETURN
       END

C ***************************************************************************

C      SUBROUTINE TO EVALUATE THE FRESNEL INTEGRALS

       SUBROUTINE DCS(C, S, X)
       IMPLICIT REAL*8 (A-H, O-Z)
       DIMENSION AA(12), BB(12), CC(12), DD(12)
       U  = X
       PIE2 = 1.5707963268D+00
       Y = PIE2 * X * X
       Z = DABS(X)
       IF(Z .NE. 0.D+00) GOTO 1000
       C = 0.D+00
       S = 0.D+00
       X = U
       RETURN
  1000 CONTINUE
       IF(Z - 4.0D+00) 3, 3, 4
     3 C = DCOS(Z)
       S = DSIN(Z)
       Z = Z / 4.0D+00
```

APPENDIX B

```
      DZ = DSQRT(Z)
      ASUM = AA(1)
      BSUM = BB(1)
      DO 40 J = 2, 12
      ASUM = ASUM + AA(J) * Z**(J -1)
      BSUM = BSUM + BB(J) * Z**(J -1)
   40 CONTINUE
      FC = DZ * ( S*BSUM +C*ASUM)
      FS = DZ * (-C*BSUM +S*ASUM)
      C = FC
      S = FS
      GOTO 5

    4 CONTINUE
      D = DCOS(Z)
      S = DSIN(Z)
      Z = 4.0D+00 / Z
      CSUM = CC(1)
      DSUM = DD(1)
      DO 30 J = 2, 12
      CSUM = CSUM +CC(J) * Z**(J -1)
   30 CONTINUE
      DSUM = DSUM +DD(J) * Z**(J -1)
      Z = DSQRT(Z)
      C = 0.5D0 +Z * (D * CSUM +S * DSUM)
      S = 0.5D0 +Z * (S * CSUM -D * DSUM)
    5 CONTINUE
      X = U
      IF(U .GT. 0.D0) GOTO 6
      C = -C
      S = -S
    6 CONTINUE
      RETURN
      DATA AA(1) , AA(2) / 0.159576914D+01  ,-0.1702D-05       /
      DATA AA(3) , AA(4) /-0.6808568854D+01 ,-0.576361D-03     /
      DATA AA(5) , AA(6) / 0.6920691902D+01 ,-0.16898657D-01   /
      DATA AA(7) , AA(8) /-0.305048566D+01  ,-0.75752419D-01   /
      DATA AA(9) , AA(10)/ 0.850663781D+00  ,-0.25639041D-01   /
      DATA AA(11), AA(12)/-0.15023096D+00   , 0.34404779D-01   /

      DATA BB(1) , BB(2) /-0.33D-07         , 0.4255387524D+01/
      DATA BB(3) , BB(4) /-0.9281D-04       ,-0.77800204D+01   /
      DATA BB(5) , BB(6) /-0.9520895D-02    , 0.5075161298D+01/
      DATA BB(7) , BB(8) /-0.138341947D+00  ,-0.1363729124D+01/
      DATA BB(9) , BB(10)/-0.403349276D+00  , 0.702222016D+00 /
      DATA BB(11), BB(12)/-0.216195929D+00  , 0.19547031D-01   /

      DATA CC(1) , CC(2) / 0.0D+00          ,-0.24933957D-01   /
      DATA CC(3) , CC(4) / 0.3936D-05       , 0.5770956D-02    /
      DATA CC(5) , CC(6) / 0.689892D-03     ,-0.9497136D-02    /
      DATA CC(7) , CC(8) / 0.11948809D-01   ,-0.6748873D-02    /
      DATA CC(9) , CC(10)/ 0.24642D-03      , 0.2102967D-02    /
      DATA CC(11), CC(12)/-0.121793D-02     , 0.233939D-03     /

      DATA DD(1) , DD(2) / 0.19947114D+00   , 0.23D-07         /
      DATA DD(3) , DD(4) /-0.9351341D-02    , 0.23006D-04      /
      DATA DD(5) , DD(6) / 0.485146D-02     , 0.1903218D-02    /
      DATA DD(7) , DD(8) /-0.17122914D-01   , 0.29064067D-01   /
      DATA DD(9) , DD(10)/-0.27928955D-01   , 0.16497308D-01   /
      DATA DD(11), DD(12)/-0.5598515D-02    , 0.9383R6D-03     /
```

Appendix C. — Computer Program DOUBLE_PLOT

```
C       PROGRAM DOUBLE_PLOT

        CHARACTER*1 DUMMY

C PROGRAM TO SET UP HT VS. dB VALUES FOR EZGRAPH

      OPEN(1, NAME = 'DOUBLEDGE.OUT', TYPE = 'OLD')
      OPEN(2, NAME = 'PLOT.DAT'     , TYPE = 'NEW')

      Q = 3001
      DO 1 I = 1, Q
         DO 3 J = 1, 23
            READ(1,99) DUMMY
3        CONTINUE
4           READ(1,*, END = 2)  FLOG, Z2
            WRITE(2,*)          FLOG, Z2
1     CONTINUE

2     CLOSE(1)
      CLOSE(2)
      STOP
99    FORMAT(A1)
      END
```

Appendix D. — Plots of Computer Studies of Doubly Diffracted Horizontally Polarized Microwaves

This appendix presents plots of horizontally polarized microwaves with the hill closer to the source set at a 15-m height and the hill farther away from the source varying in height from 5 to 45 m.

These figures show the effect of terrain on a source with nonuniform antenna gain. Gain of power density relative to free space is shown in decibel scale versus target height.

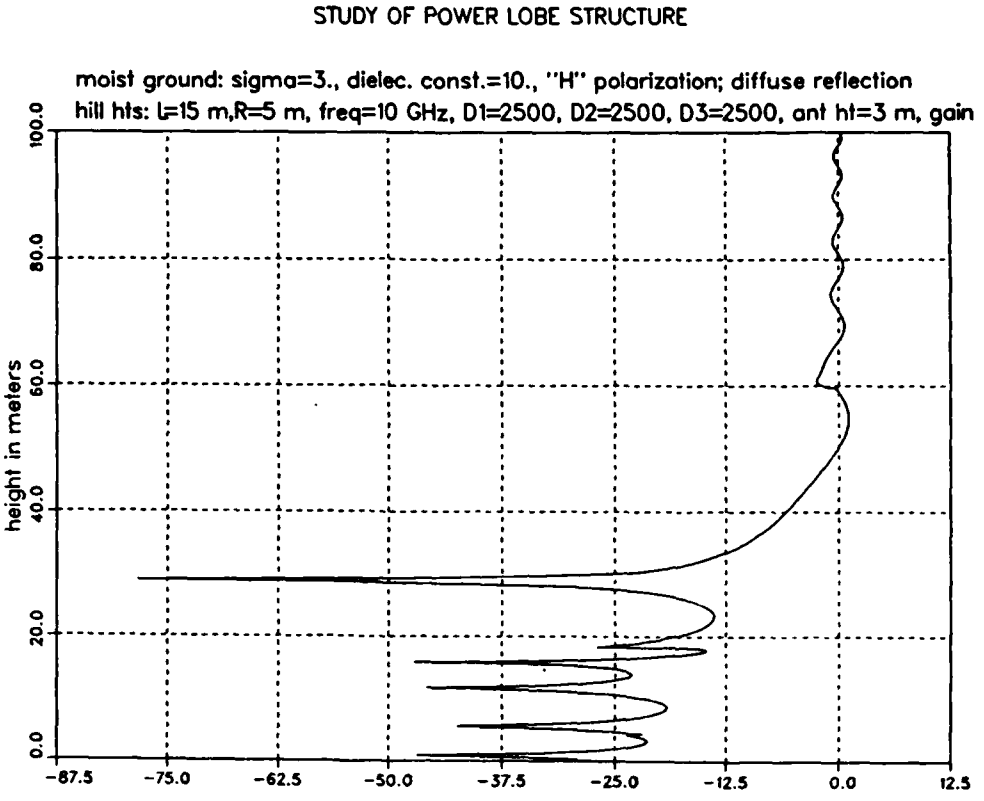

Figure D-1. Case of hill 15 m high near source and hill 5 m high near target, with horizontal polarization. Antenna height is 3 m.

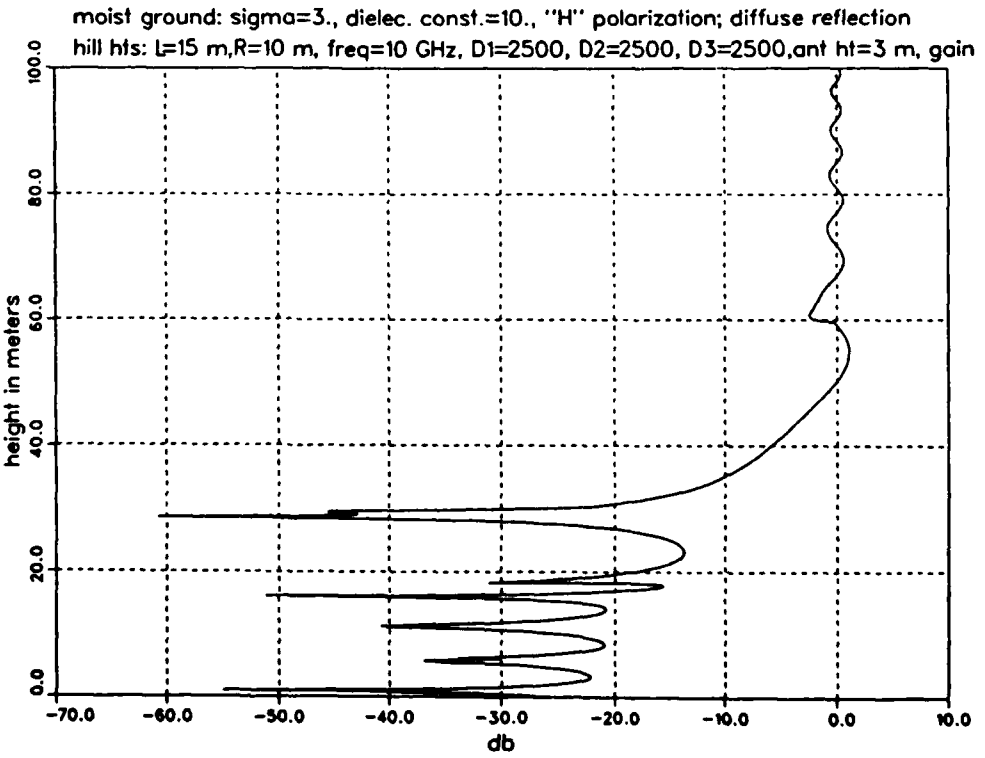

Figure D-2. Case of hill 15 m high near source and hill 10 m high near target, with horizontal polarization. Antenna height is 3 m.

APPENDIX D

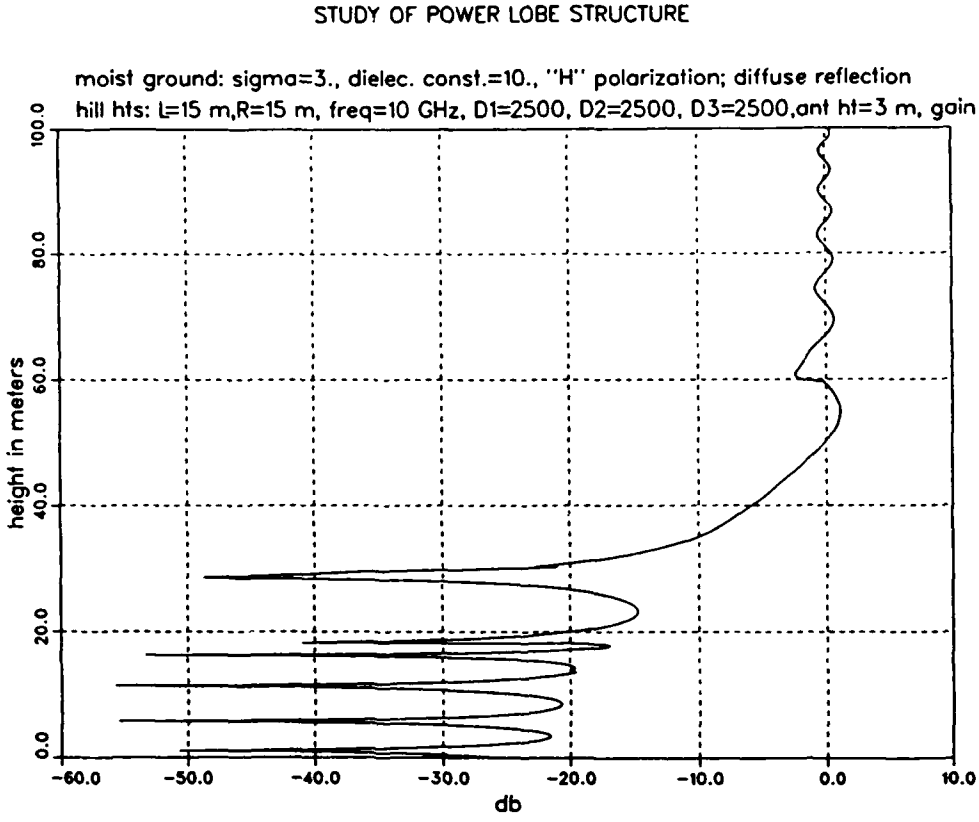

Figure D-3. Case of hill 15 m high near source and hill 15 m high near target, with horizontal polarization. Antenna height is 3 m.

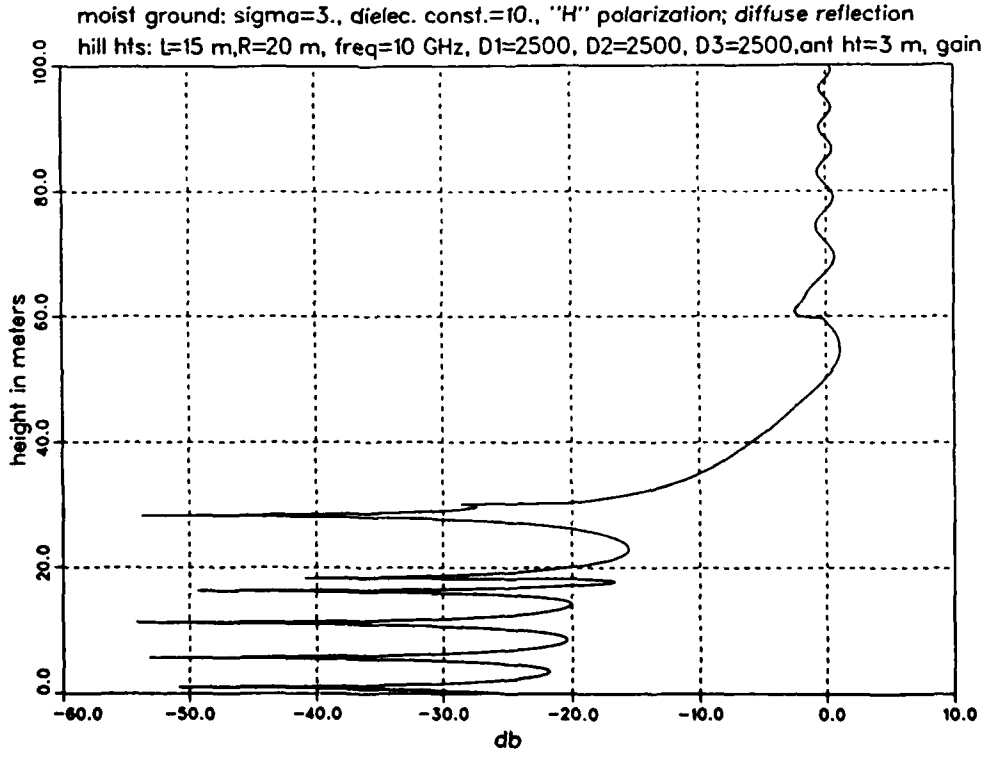

Figure D-4. Case of hill 15 m high near source and hill 20 m high near target, with horizontal polarization. Antenna height is 3 m.

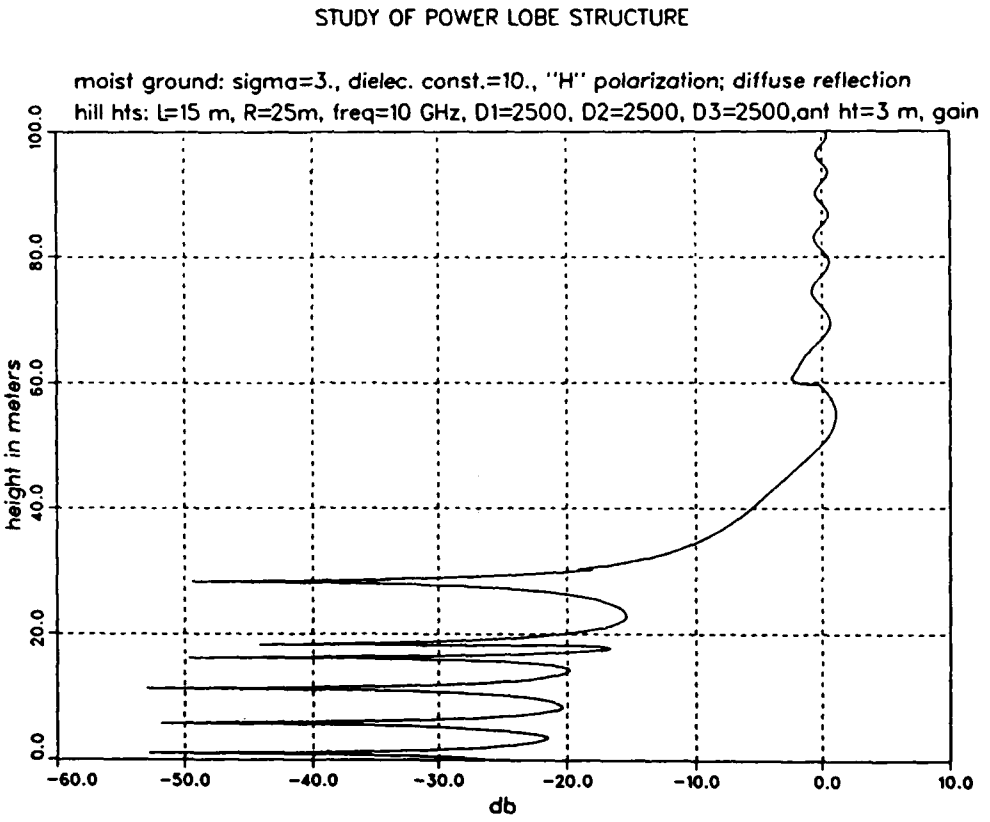

Figure D-5. Case of hill 15 m high near source and hill 25 m high near target, with horizontal polarization. Antenna height is 3 m.

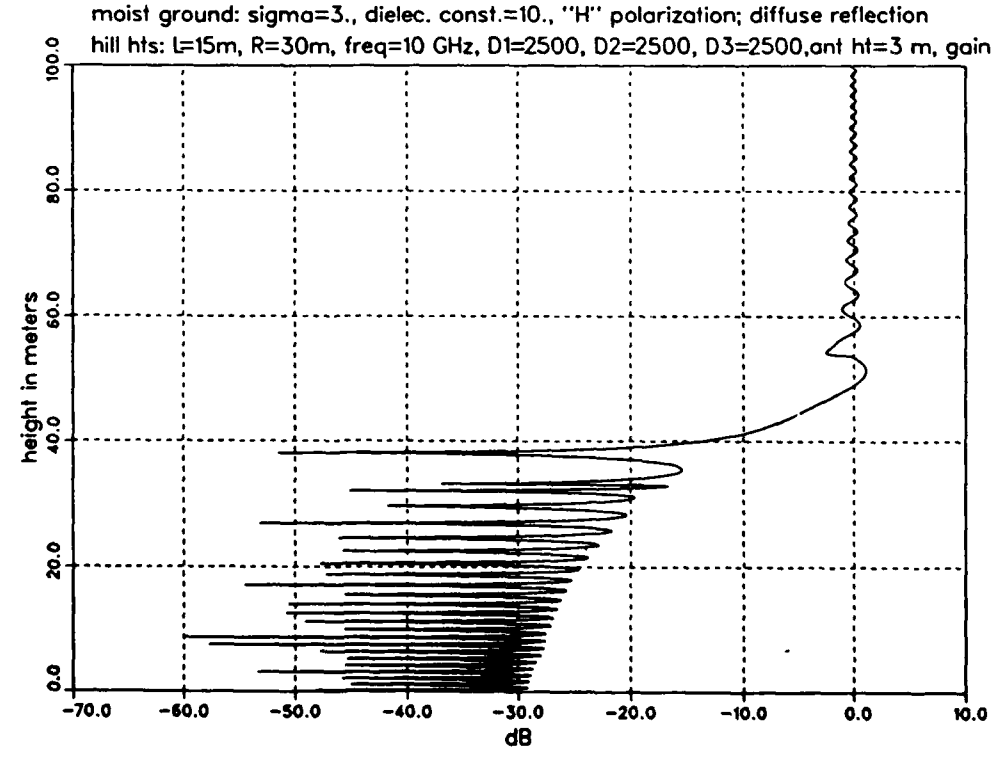

Figure D-6. Case of hill 15 m high near source and hill 30 m high near target, with horizontal polarization. Antenna height is 3 m.

APPENDIX D

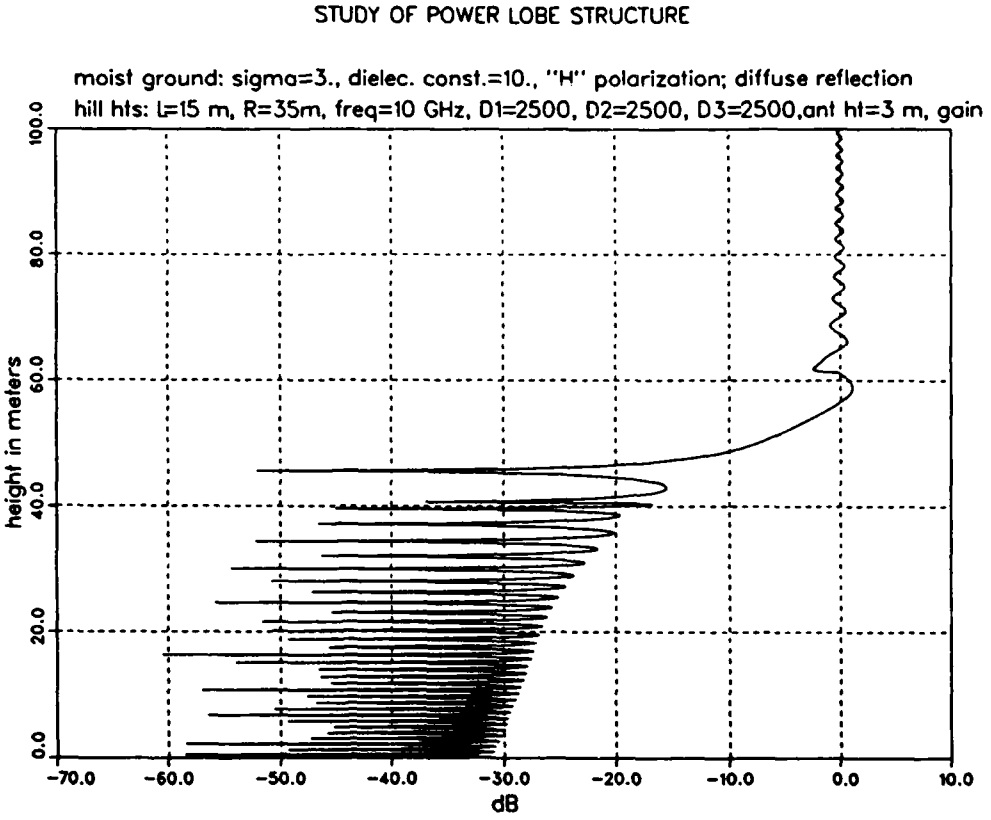

Figure D-7. Case of hill 15 m high near source and hill 35 m high near target, with horizontal polarization. Antenna height is 3 m.

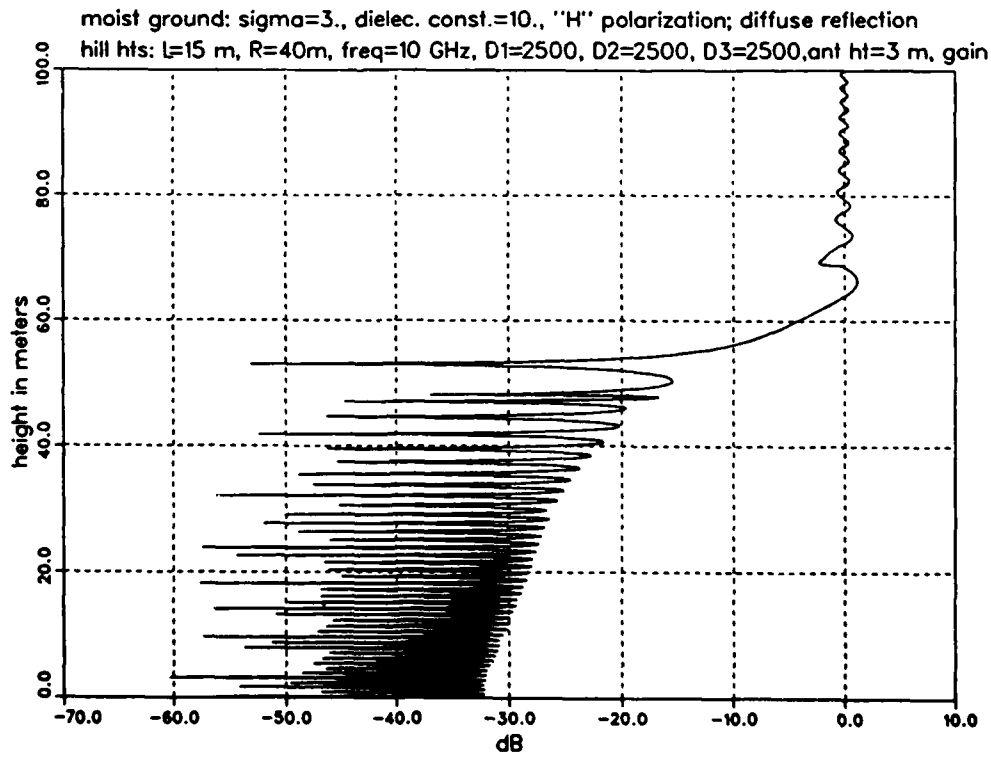

Figure D-8. Case of hill 15 m high near source and hill 40 m high near target, with horizontal polarization. Antenna height is 3 m.

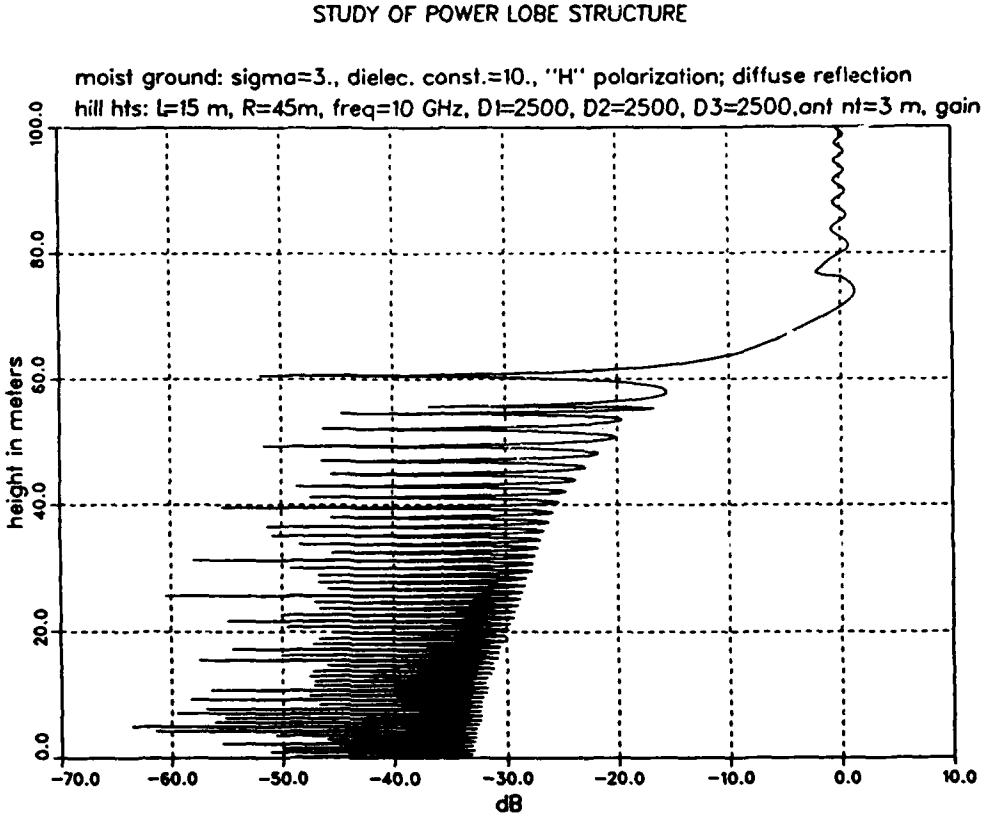

Figure D-9. Case of hill 15 m high near source and hill 45 m high near target, with horizontal polarization. Antenna height is 3 m.

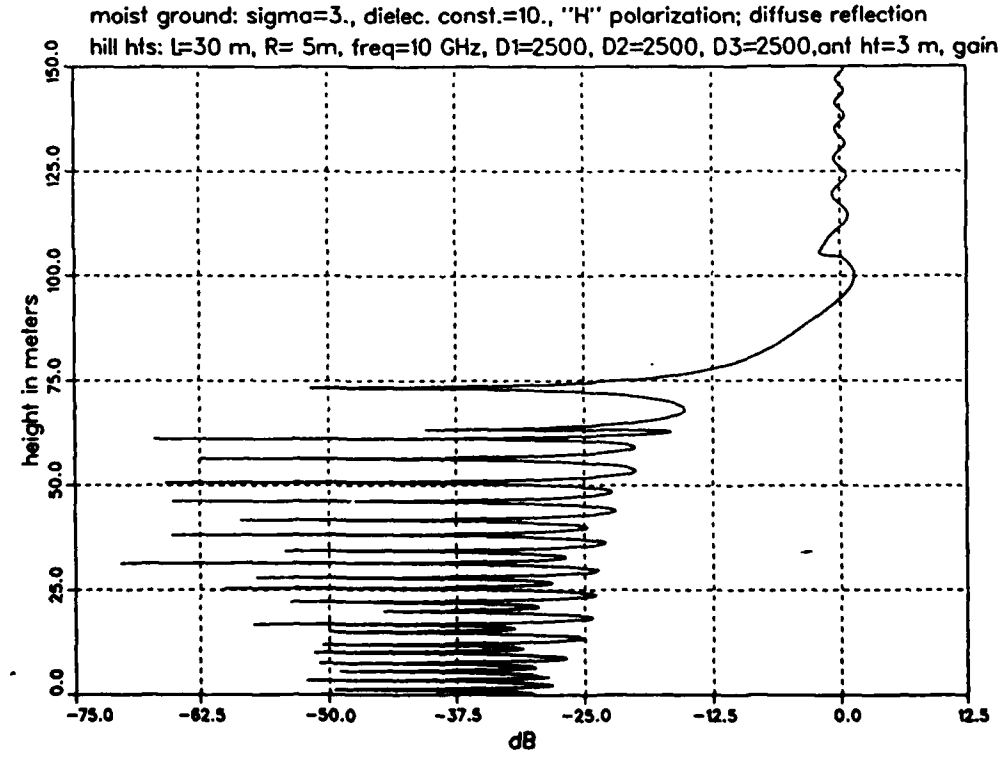

Figure D-10. Case of hill 30 m high near source and hill 5 m high near target, with horizontal polarization. Antenna height is 3 m.

APPENDIX D

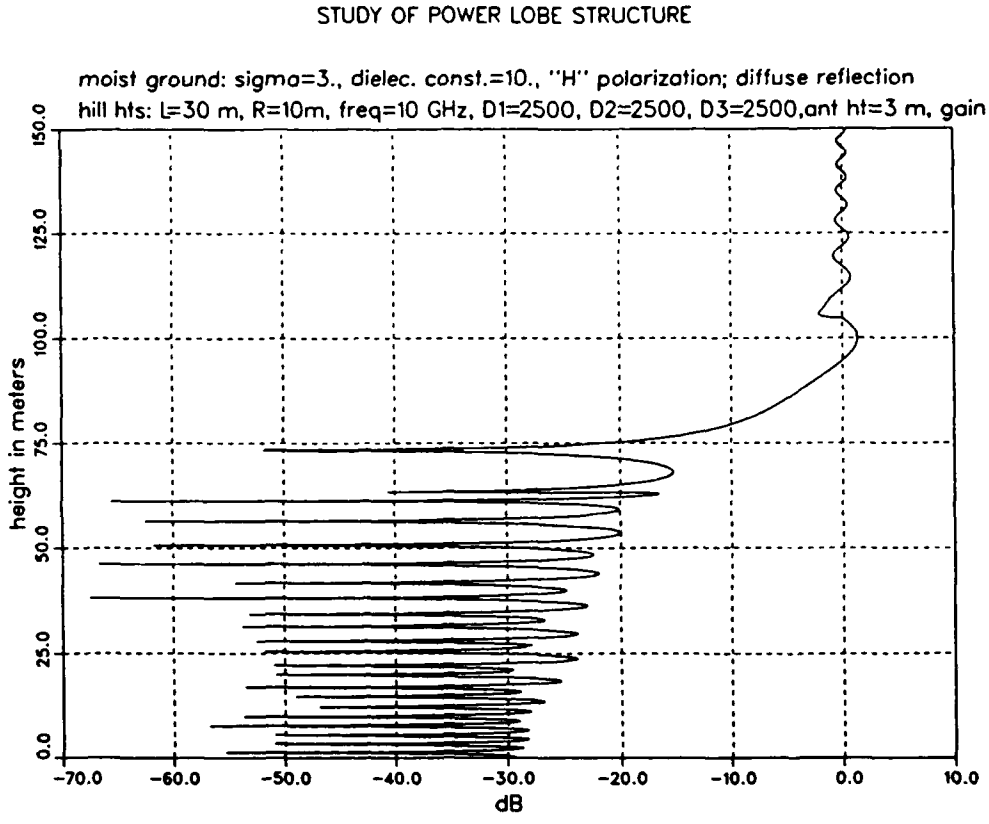

Figure D-11. Case of hill 30 m high near source and hill 10 m high near target, with horizontal polarization. Antenna height is 3 m.

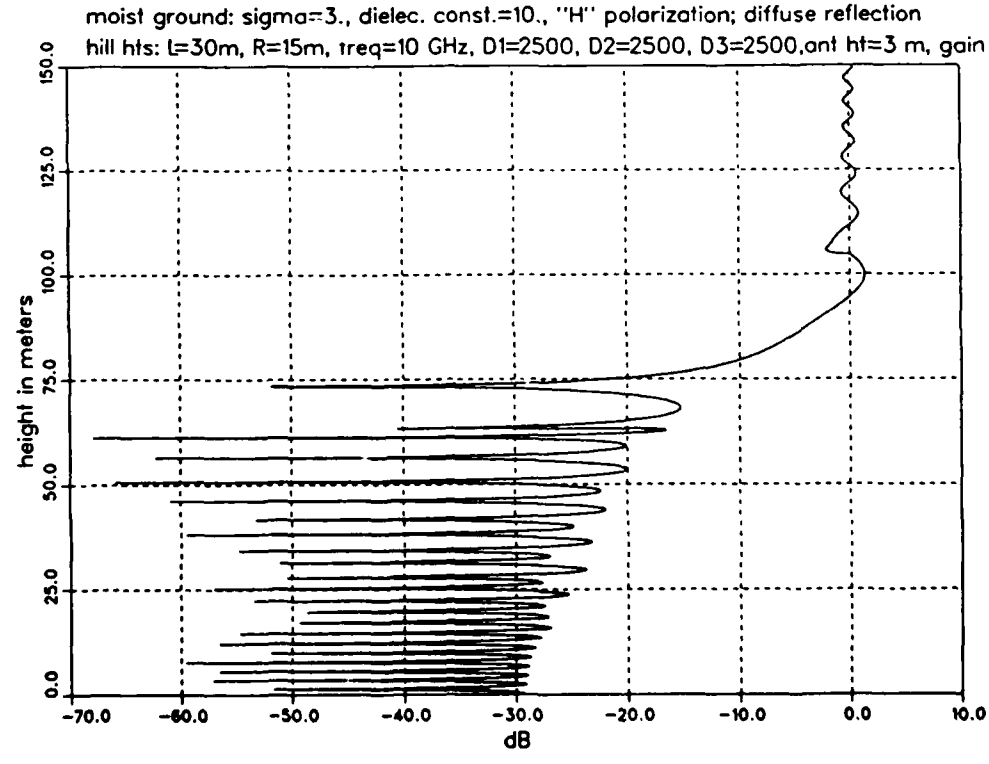

Figure D-12. Case of hill 30 m high near source and hill 15 m high near target, with horizontal polarization. Antenna height is 3 m.

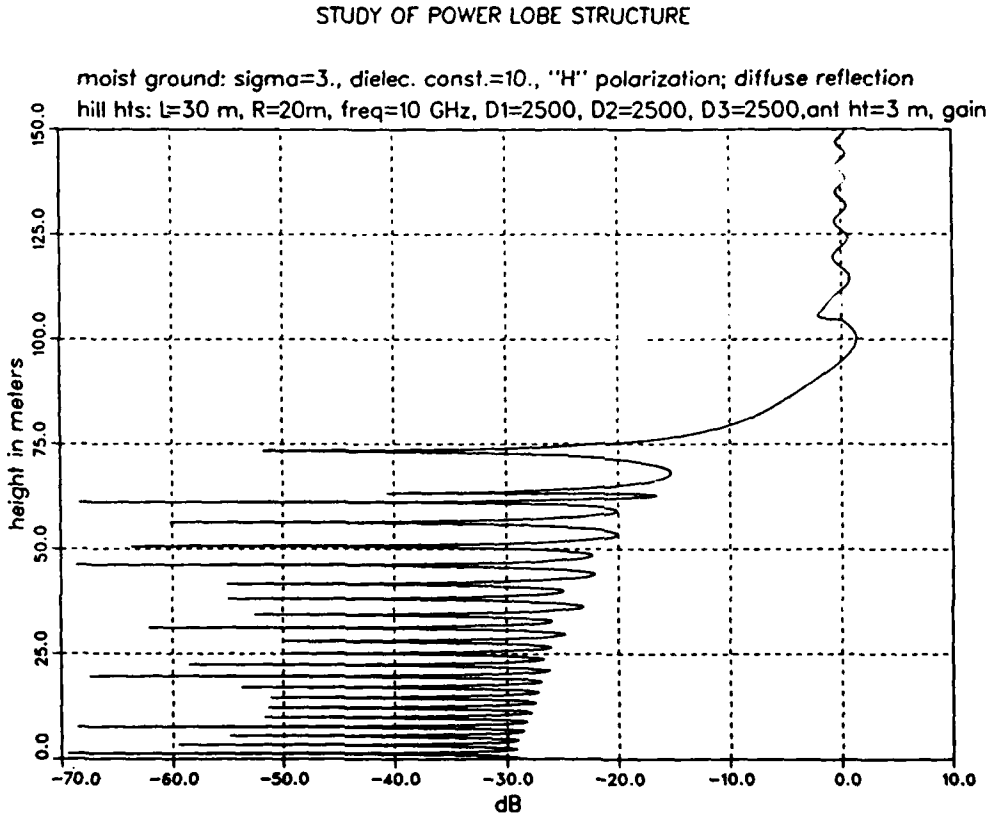

Figure D-13. Case of hill 30 m high near source and hill 20 m high near target, with horizontal polarization. Antenna height is 3 m.

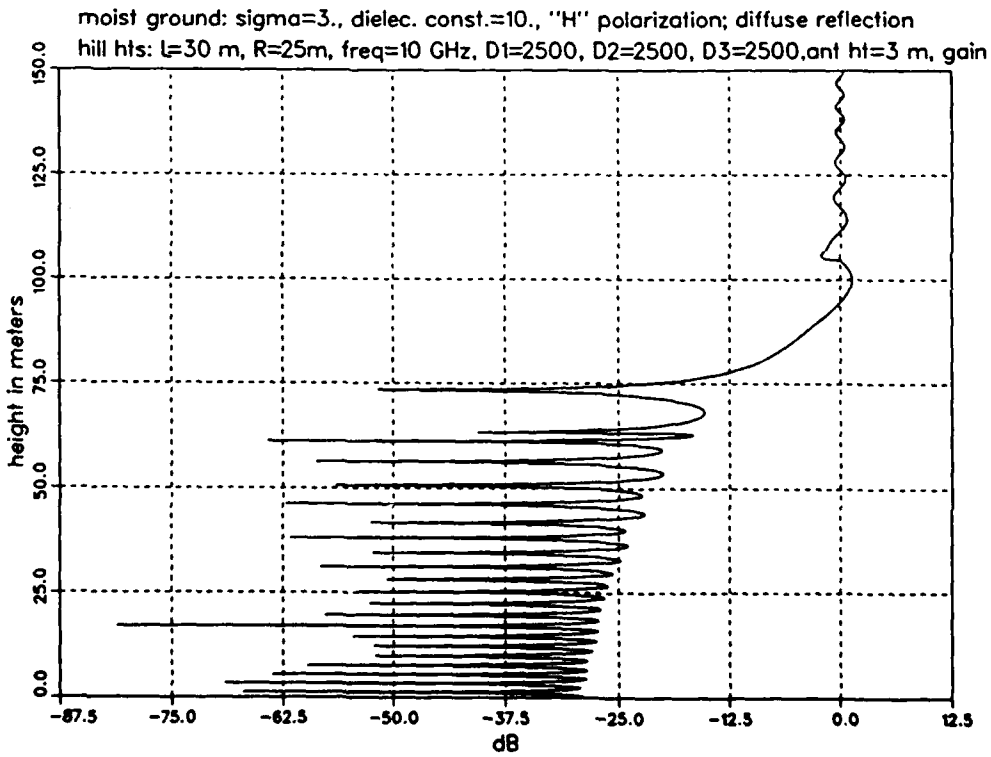

Figure D-14. Case of hill 30 m high near source and hill 25 m high near target, with horizontal polarization. Antenna height is 3 m.

APPENDIX D

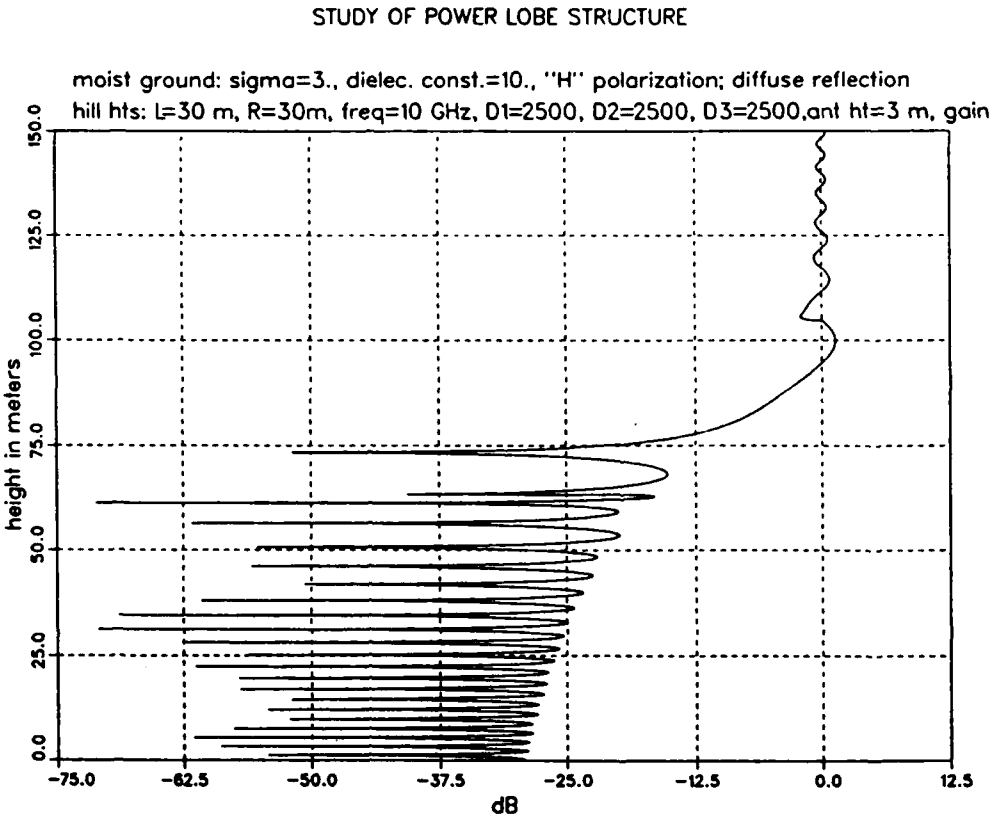

Figure D-15. Case of hill 30 m high near source and hill 30 m high near target, with horizontal polarization. Antenna height is 3 m.

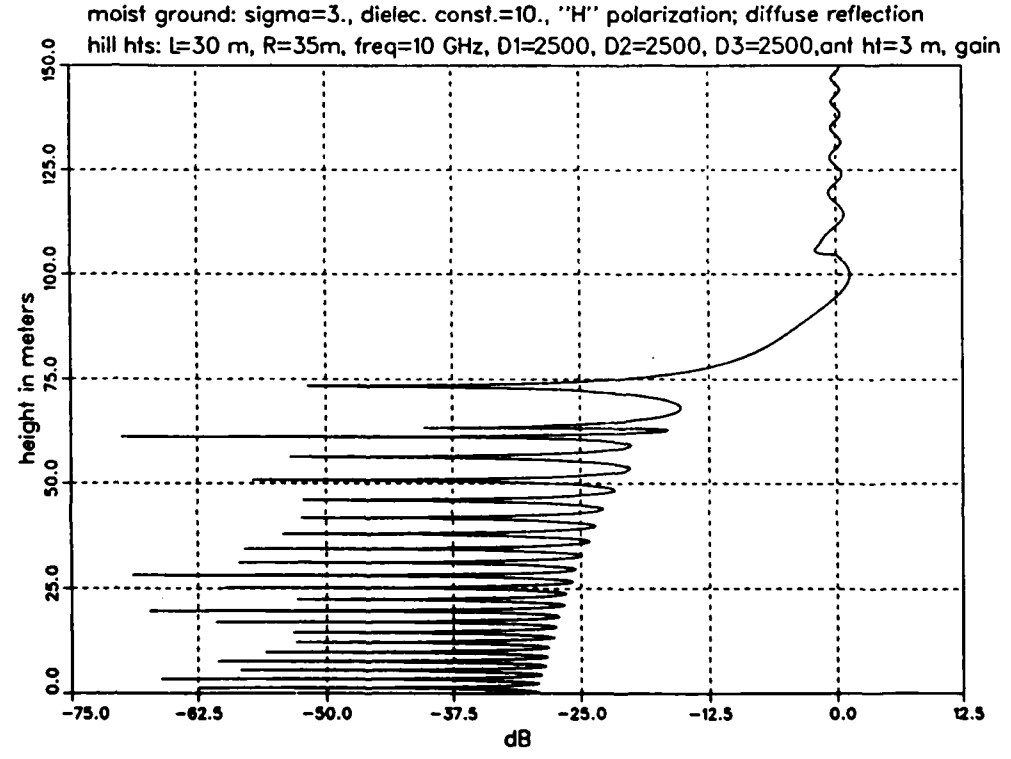

Figure D-16. Case of hill 30 m high near source and hill 35 m high near target, with horizontal polarization. Antenna height is 3 m.

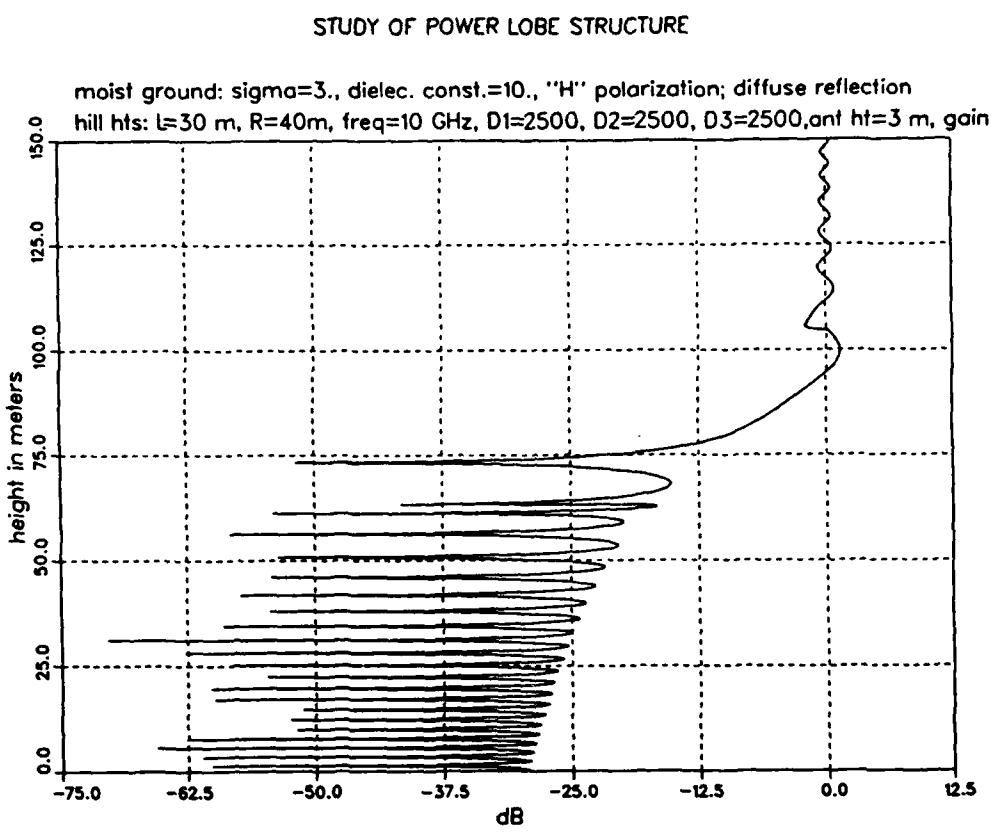

Figure D-17. Case of hill 30 m high near source and hill 40 m high near target, with horizontal polarization. Antenna height is 3 m.

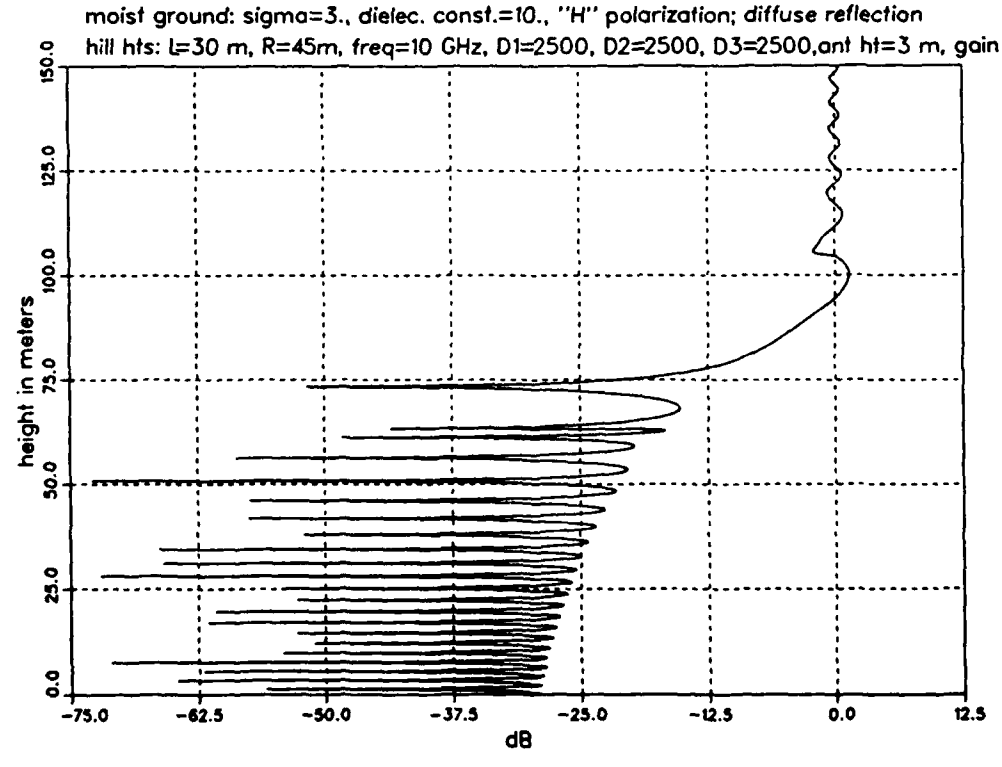

Figure D-18. Case of hill 30 m high near source and hill 45 m high near target, with horizontal polarization. Antenna height is 3 m.

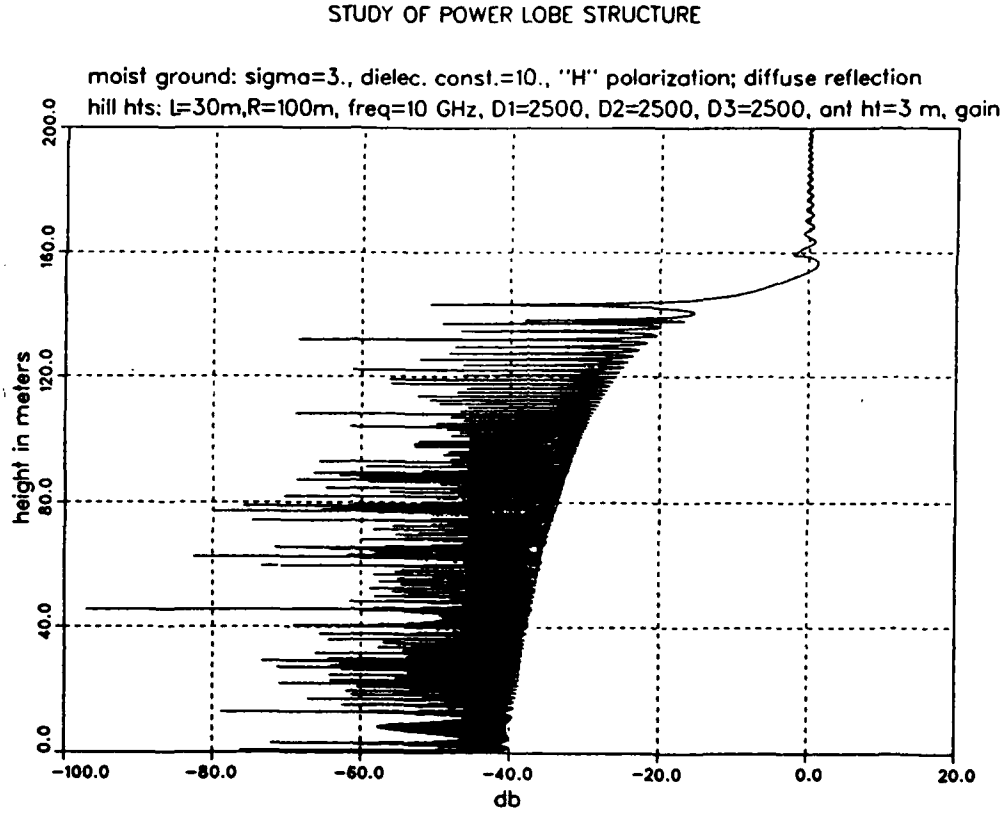

Figure D-19. Case of hill 30 m high near source and hill 100 m high near target, with horizontal polarization. Antenna height is 3 m.

Appendix E. — Power Density Comparison Plots at Target:
(1) Double Diffraction Versus Single Diffraction (fig. E-1 to E-3)
and
(2) Transmitter Height of 3 m Versus 6m (fig. E-4 to E-7)

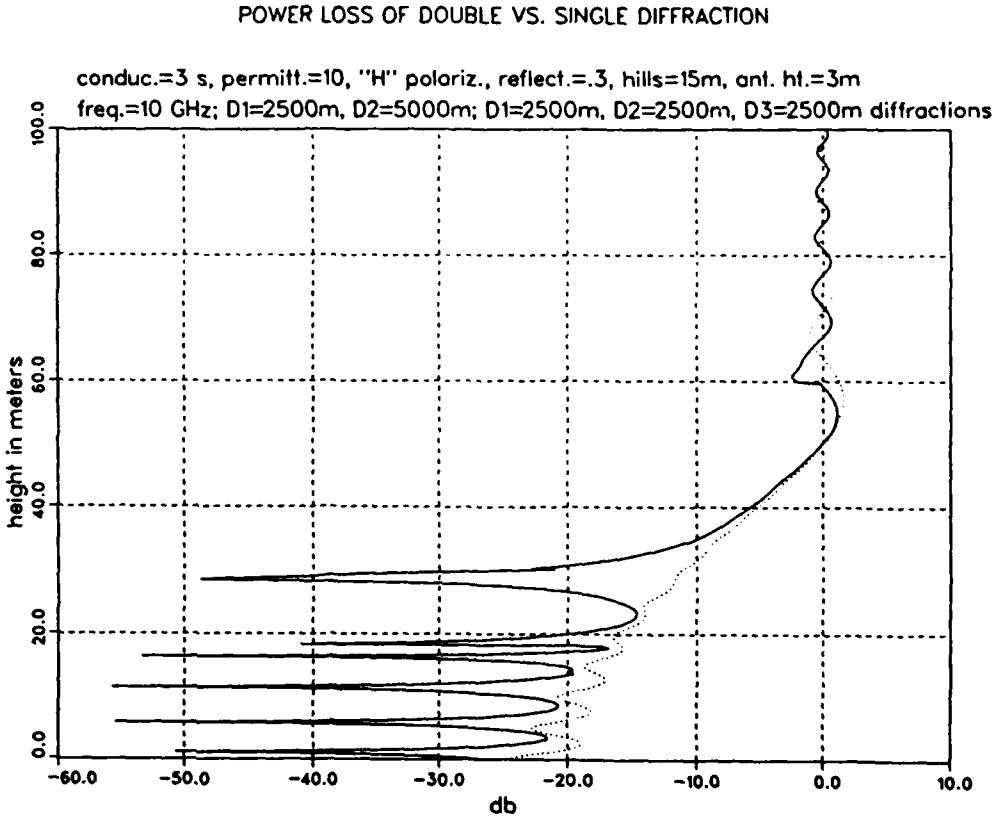

Figure E-1. Comparison (over electrically interactive terrain) of power density loss from diffraction over two edges to power density loss resulting from diffraction over one edge. Positive or negative gain in decibel units is measured relative to free space propagation at 0 dB. In this case, single edge is set closer to microwave emitter than to target.

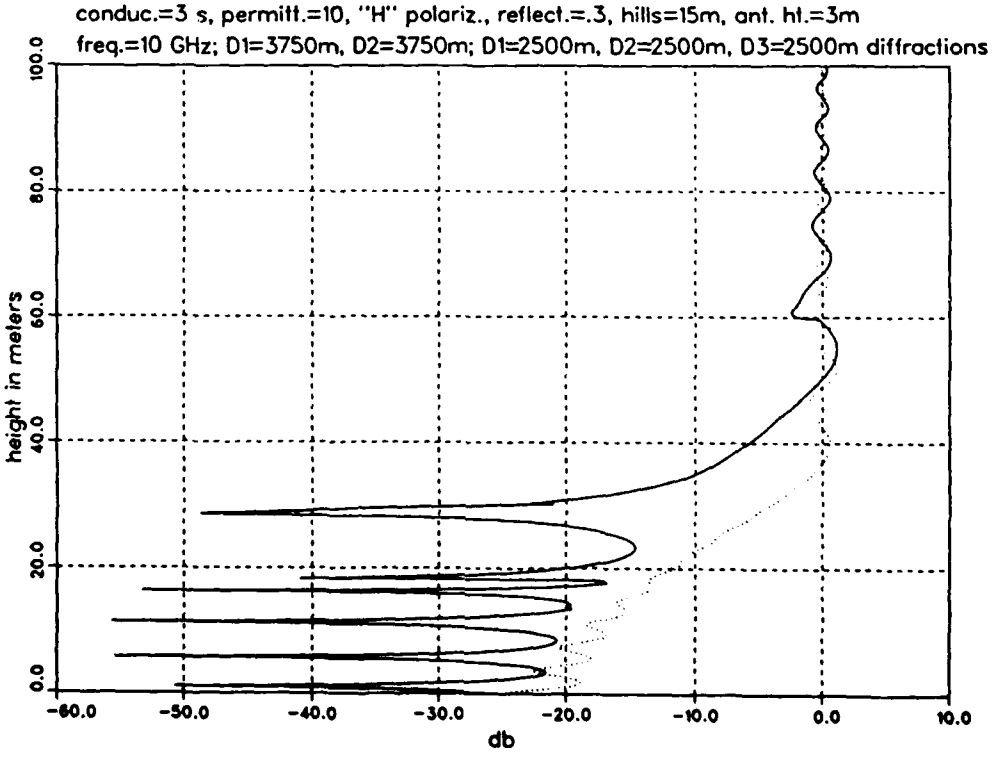

Figure E-2. Comparison (over electrically interactive terrain) of power density loss from diffraction over two edges to power density loss resulting from diffraction over one edge. Positive or negative gain in decibel units is measured relative to free space propagation at 0 dB. In this case, single edge is set midway between emitter and target.

APPENDIX E

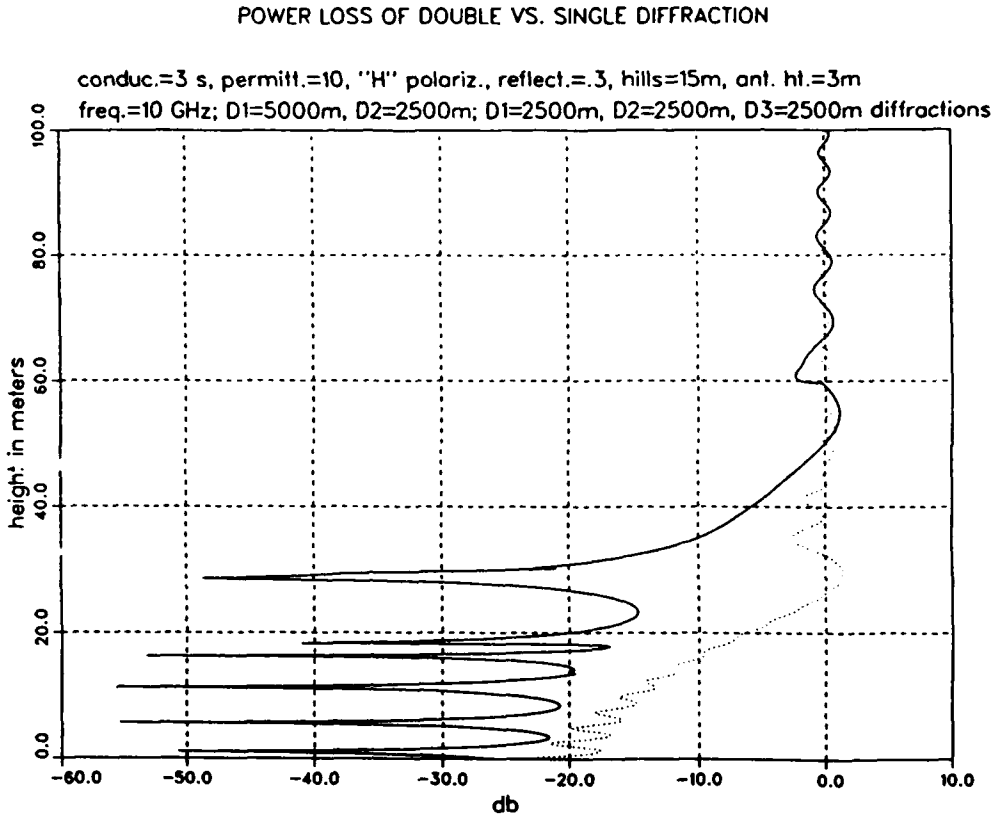

Figure E-3. Comparison (over electrically interactive terrain) of power density loss from diffraction over two edges to power density loss resulting from diffraction over one edge. Positive or negative gain in decibel units is measured relative to free space propagation at 0 dB. In this case, single edge is set closer to target than to microwave emitter.

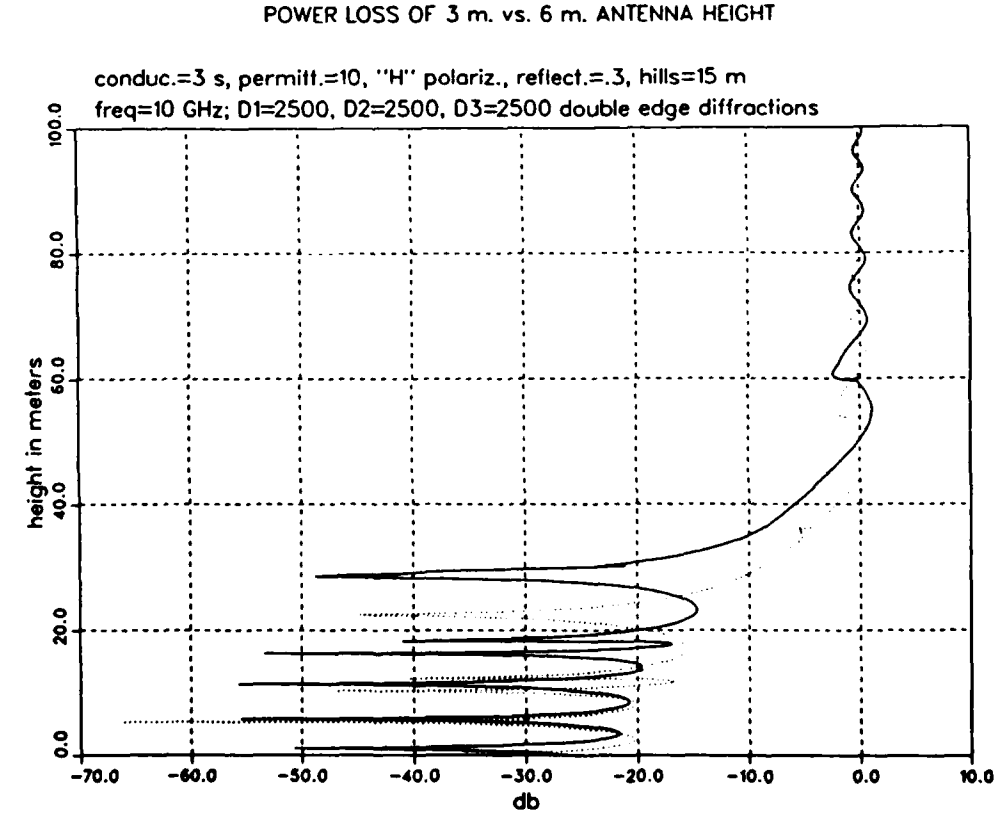

Figure E-4. Comparison (over electrically interactive terrain) of power density loss from diffraction over two 15-m-high edges for microwave emitters set at heights of 3 and 6 m, respectively. Solid curve shows antenna height at 3 m, and dotted curve, at 6 m.

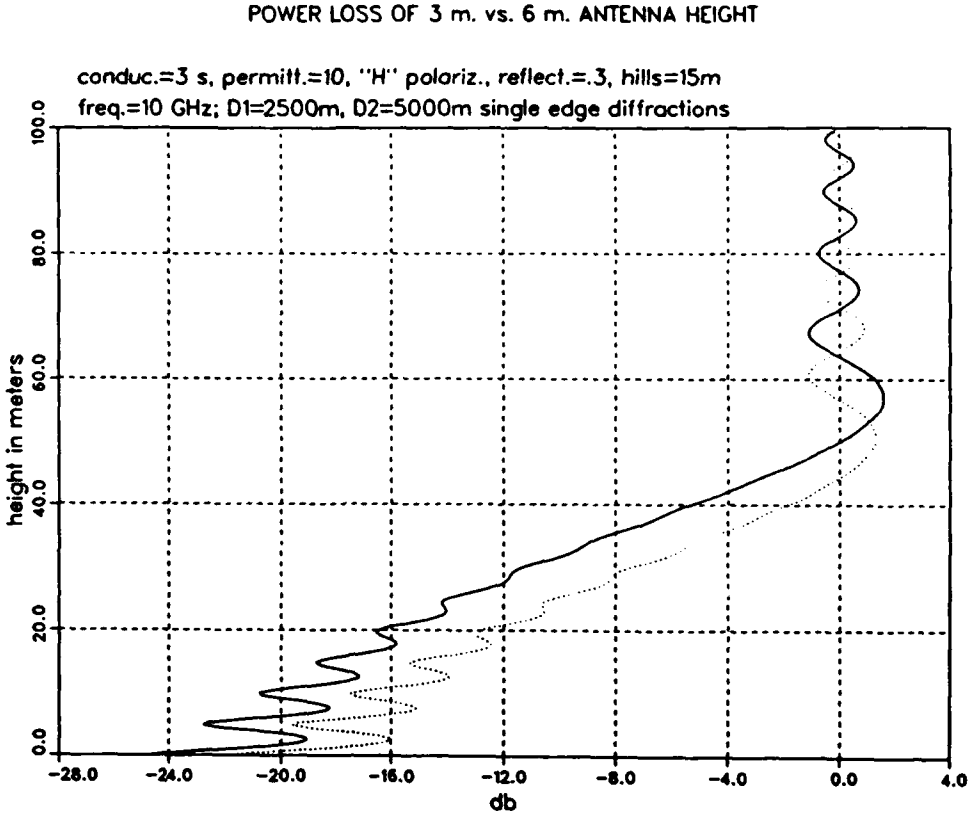

Figure E-5. Comparison (over electrically interactive terrain) of power density loss from diffraction over a single knife edge set at a 15-m height to microwave emitters set at 3- and 6-m heights, respectively. Solid curve shows antenna height at 3 m, and dotted curve, at 6 m. Edge is here set closer to emitters than it is to target.

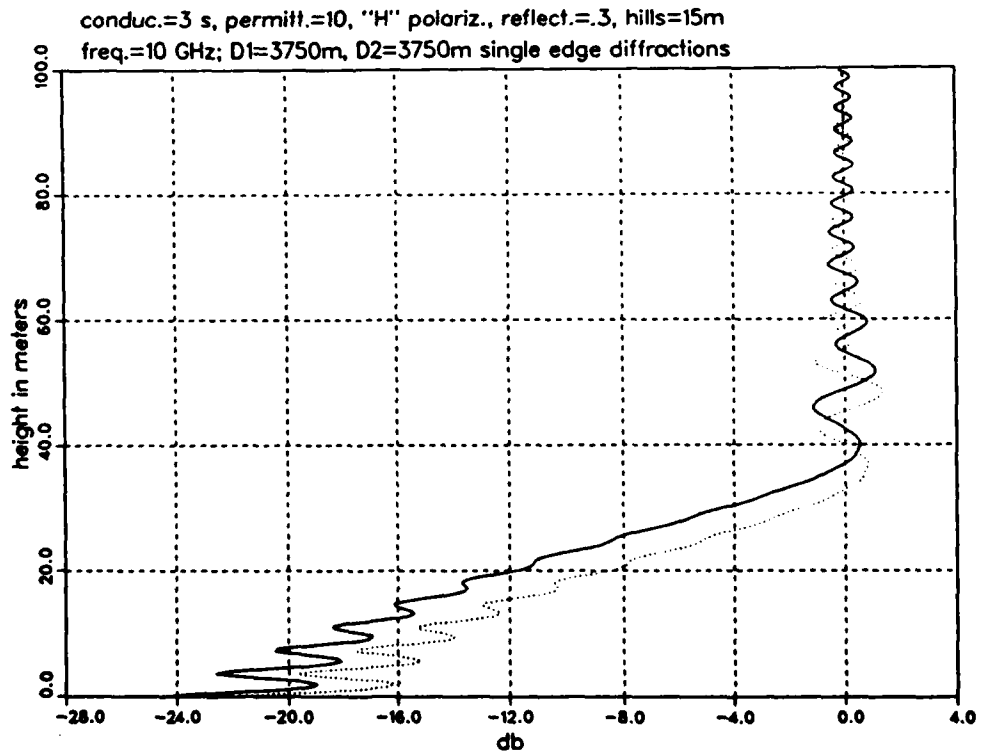

Figure E-6. Comparison (over electrically interactive terrain) of power density loss from diffraction over a single knife edge set at a 15-m height to microwave emitters set at 3- and 6-m heights, respectively. Solid curve shows antenna height at 3 m, and dotted curve, at 6 m. Edge is here set midway between emitters and target.

APPENDIX E

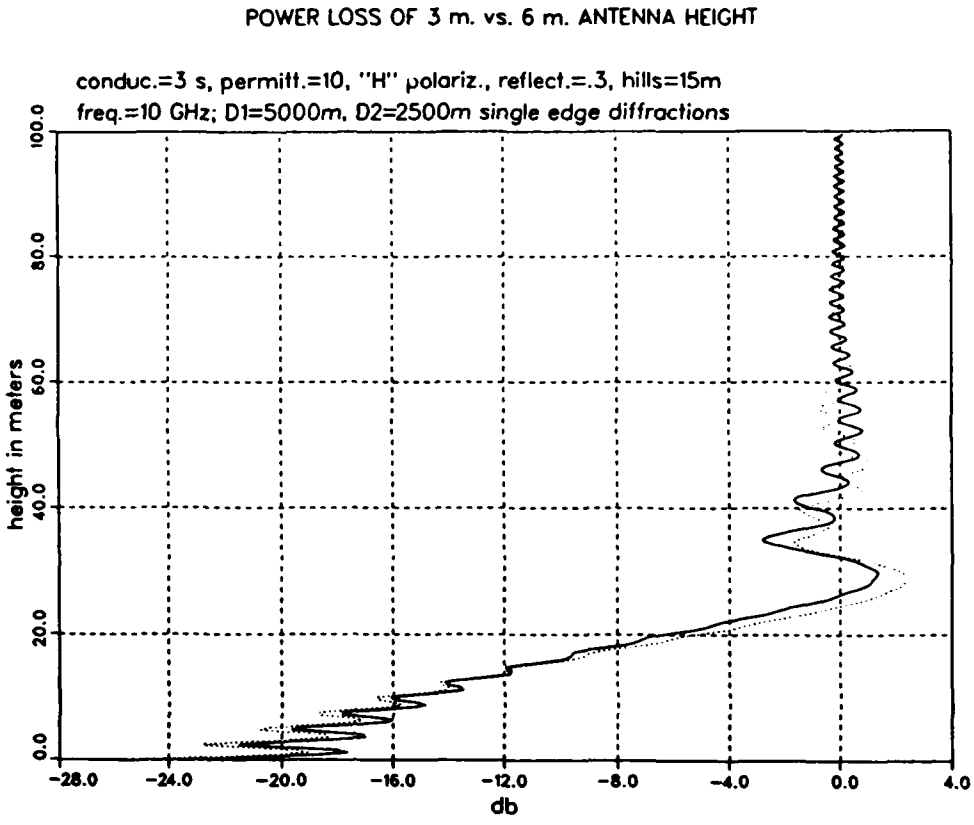

Figure E-7. Comparison (over electrically interactive terrain) of power density loss from diffraction over a single knife edge set at a 15-m height to microwave emitters set at 3- and 6-m heights, respectively. Solid curve shows antenna height at 3 m, and dotted curve, at 6 m. Edge is here set closer to target than to microwave emitters.

Appendix F. — Plot Comparing a Theoretically Derived Curve for Two Diffractions over Terrain with a Curve Prepared from Field Measurement Data for Two Diffractions over Terrain

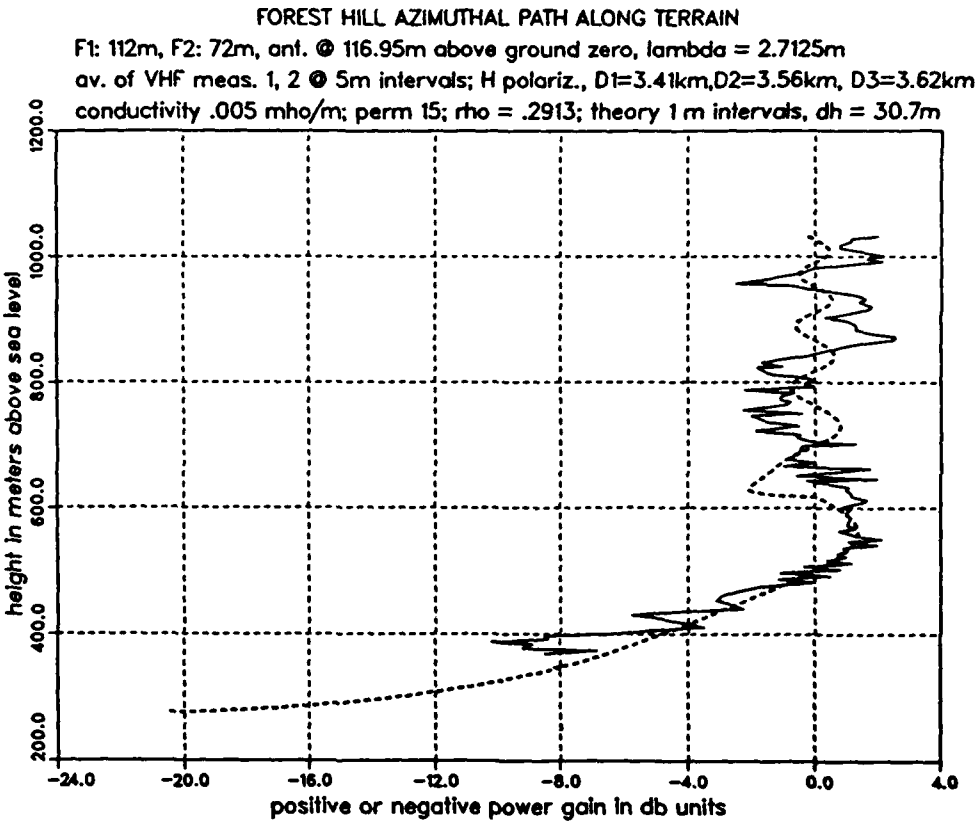

Figure F-1. Comparison of theoretically derived curve for two consecutive diffractions with curve derived from field measurement data for signal transmission over two peaks. Path is Forest Hill azimuth relative to transmitter. Transmitter is 392.95 m above sea level; ground zero is 276 m above sea level.

Appendix G. — Plot Comparing a Theoretically Derived Curve for a Single Diffraction over Terrain (using the KNIFEDGE Program) with a Curve Prepared from Field Measurement Data for Two Diffractions over Terrain

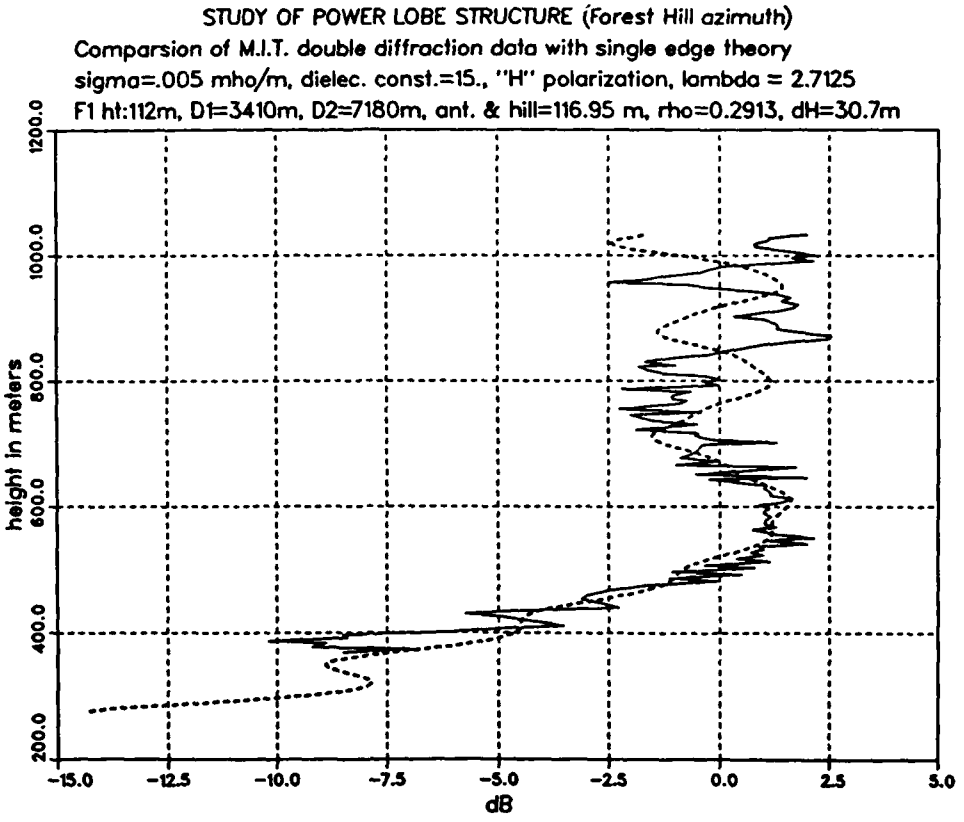

Figure G-1. Comparison of theoretically derived curve for a single diffraction with curve derived from field measurement data for signal transmission over two peaks. Path is Forest Hill azimuth relative to transmitter. Transmitter is 392.95 m above sea level; ground zero is 276 m above sea level.

DISTRIBUTION

ADMINISTRATOR
DEFENSE TECHNICAL INFORMATION
CENTER
ATTN DTIC-DDA (12 COPIES)
CAMERON STATION, BUILDING 5
ALEXANDRIA, VA 22304-6145

DEFENSE NUCLEAR AGENCY
ATTN G. KWITKOSKI
ATTN J. BACHKOSKY
ATTN J. PIERRE
WASHINGTON, DC 20305-1000

DEFENSE INTELLIGENCE AGENCY
ATTN DC-D, COL R. M. ATCHISON
WASHINGTON, DC 20301

MR. L. HURZON
PO BOX 1925
WASHINGTON, DC 20013

HEADQUARTERS
DEPT OF THE ARMY
ATTN DAMO-FDI, LTC D. HEARN
ATTN DAMO-FDI, LTC J. RILEY
ATTN SARD-ZT, H. WOODALL
ATTN DACS(DMP), LTC M. TOCH
ATTN DAMO-FDI, COL M. M. PARRILLI
ATTN SARD-SS, LTC PURDIN
ATTN SARD-TNS, DR. J. B. STEKERT
WASHINGTON, DC 20310

HEADQUARTERS
US ARMY ARMAMENT RESEARCH,
DEVELOPMENT, & ENGR CENTER
ATTN SMCAR-AE, G. TAYLOR
PICATINNY ARSENAL, NJ 07806-5000

BALLISTIC RESEARCH LABORATORY
ATTN SLCBR-VL-I, J. E. KAMMERER
ABERDEEN PROVING GROUND, MD 21005-5066

US ARMY BELVOIR RESEARCH DEVELOPMENT
& ENGINEERING CENTER
ATTN STRBE-FGE, L. I. AMSTUTZ
ATTN D. C. HEBERLEIN
ATTN STRBE-JC, J. OWEN
FT BELVOIR, VA 22060-5606

US ARMY CENTER FOR SIGNALS WARFARE
ATTN DIRECTOR, H. S. HOVEY, JR
VINT HILL FARMS STATION
WARRENTON, VA 22186-5100

US ARMY COMBINED ARMS CENTER
ATTN ATZL-SCT, J. FOX
ATTN ATZL-CAP, COL J. HENDERSON
ATTN ATZL-CAP/D, MAJ M. McKEE
ATTN ATZL-CAP/D, MAJ K. PECHAK

US ARMY COMBINED ARMS CENTER (cont'd)
ATTN ATZL-CAP/D, LTC O. STOKES
FT LEAVENWORTH, KS 66017-5000

DARPA
ATTN TTO, J. ENTZMINGER
ATTN DEO, L. BUCHANAN
1400 WILSON BLVD
ARLINGTON, VA 22209

ELECTRONICS TECHNOLOGY AND
DEVICES LAB

ATTN SLCET-ML, S. LEVY
ATTN SLCET-D, C. THORNTON
FT MONMOUTH, NJ 07719-5000

HEADQUARTERS
INSCOM
ATTN COL S. SEMERLY
ATTN MAJ R. JACKSON
ARLINGTON HALL STATION
ARLINGTON, VA 22120

US ARMY MATERIEL SYS ANAL AGENCY
ATTN AMXSY-CS, P. BEAVERS
ABERDEEN PROVING GROUND, MD 21005

HEADQUARTERS
US ARMY MATERIEL COMMAND
ATTN AMCDRA, R. O. BLACK
ATTN AMCPEO-AM-MS, L. STANTON
ATTN AMCPEO-AM-MS, LTC K. STARR
5001 EISENHOWER AVENUE
ALEXANDRIA, VA 22333-0001

US ARMY MISSILE COMMAND
ATTN DRSMI-RD-DE, E. B. JENNINGS
ATTN DRSMI-RD-DE, R. CONRAD
ATTN DRSMI-RD-DE, B. JACKSON
REDSTONE ARSENAL, AL 35898-5000

OUSDA (R&AT/EST)
ATTN MR. D. N. FREDERICKSEN
ATTN COL B. D. CRANE
ATTN J. MacCALLUM
ATTN W. SNOWDEN
WASHINGTON, DC 20301-5000

US ARMY TRAINING & DOCTRINE COMMAND
ATTN ATCD-G, J. M. GRAY
FT MONROE, VA 23651

VULNERABILITY ASSESSMENT LABORATORY
ATTN SLCVA-TAC, D. ALVAREZ
WHITE SANDS MISSILE RANGE, NM 88002

DISTRIBUTION (cont'd)

HEADQUARTERS
DEPARTMENT OF THE NAVY
ATTN OP-987, F. SHOUP
ATTN OP-50W3, LT C. SPRINKLE
ATTN OP-076, G. WORKMAN
WASHINGTON, DC 20350

NAVAL RESEARCH LABORATORY
ATTN T. WEITING
ATTN W. ELLIS
ATTN D. NAGEL
ATTN W. MANHEIMER
4555 OVERLOOK AVENUE, SW
WASHINGTON, DC 20375

NAVAL SURFACE WEAPONS CENTER
ATTN J. TINO, HEAD, PROTECTION
SYSTEMS DEPARTMENT H
ATTN J. F. GOFF, R301 HEAD, MATERIALS
APPLICATIONS OFFICE
ATTN D. LYNCH, H21, BUILDING 130
ATTN J. GOELLER, V02 DEPUTY DEPARTMENT
HEAD, UNDERWATER SYSTEMS DEPT
ATTN R. WOODHAM, U31, BUILDING 4
ATTN D. GIBSON, U31, BUILDING 4
ATTN G. GAUNAURD, R43
SILVER SPRING, MD 20903-5000

SPACE AND NAVAL WARFARE
SYSTEMS COMMAND
ATTN PMW-145, CPT J. D. FONTANA
ATTN PMW-145, CDR M. KAISER
WASHINGTON, DC 20363-5100

HEADQUARTERS
DEPARTMENT OF THE AIR FORCE
ATTN AFCSA/SGRA, MAJ R. L. EILERS
WASHINGTON, DC 20330

US AIR FORCE SYSTEMS COMMAND
ATTN AFSC/XTWT, LTCOL W. DUNGAN
ANDREWS AFB, MD 20334-5000

AIR FORCE WEAPONS LABORATORY
ATTN AFWL/AWP, W. L. BAKER
KIRTLAND AFB, NM 87117-6008

MARINE CORPS DEV CENTER
FIREPOWER DIV (D-094)
ATTN LTC H. L. MAY
QUANTICO, VA 22134

NASA
GODDARD SPACE FLIGHT CENTER
ATTN J. SIRY, CODE 671, BLDG 22
GREENBELT, MD 20771

FOREIGN SCIENCE & TECHNOLOGY
CENTER
ATTN AIAST-RA-ST1, T. CALDWELL
220 SEVENTH STREET NE
CHARLOTTESVILLE, VA 22901

LAWRENCE LIVERMORE NATIONAL LAB
ATTN H. S. CABAYAN
ATTN D. J. CHASE
PO BOX 5504
LIVERMORE, CA 94550

LOS ALAMOS NATIONAL LAB
ATTN DR. J. TOEVS, MS 5000
ATTN R. F. HOBERLING, MS F668
PO BOX 1663
LOS ALAMOS, NM 87545

SANDIA NATIONAL LAB
ATTN J. HOFFMAN, DIV 1236
ATTN J. POWELL, DIV 1230
PO BOX 5800
ALBUQUERQUE, NM 87185

US ARMY LABORATORY COMMAND
ATTN TECHNICAL DIRECTOR, AMSLC-TD

INSTALLATION SUPPORT ACTIVITY
ATTN LEGAL OFFICE, SLCIS-CC

USAISC
ATTN RECORD COPY, AMSLC-IM-TS
ATTN TECHNICAL REPORTS BRANCH,
AMSLC-IM-TR (2 COPIES)

HARRY DIAMOND LABORATORIES
ATTN DIRECTOR, SLCHD-D
ATTN DIVISION DIRECTORS
ATTN DIVISION DIRECTOR, SLCHD-NW
ATTN LIBRARY, SLCHD-TL (3 COPIES)
ATTN LIBRARY, SLCHD-TL (WOODBRIDGE)
ATTN CHIEF, SLCHD-NW-E
ATTN CHIEF, SLCHD-NW-RP
ATTN CHIEF, SLCHD-NW-EH
ATTN CHIEF, SLCHD-NW-ES
ATTN CHIEF, SLCHD-NW-R
ATTN CHIEF, SLCHD-NW-TN
ATTN CHIEF, SLCHD-NW-RP
ATTN CHIEF, SLCHD-NW-CS
ATTN CHIEF, SLCHD-NW-TS
ATTN CHIEF, SLCHD-NW-RS
ATTN CHIEF, SLCHD-NW-P
ATTN E. BROWN, SLCHD-HPM
ATTN S. GRAYBILL, SLCHD-HPM
ATTN R. GARVER, SLCHD-NW-CS
ATTN S. HAYES, SLCHD-NW-CS

HARRY DIAMOND LABORATORIES (cont'd)
ATTN S. SADDOW, SLCHD-NW-CS
ATTN J. TATUM, SLCHD-NW-CS
ATTN H. BRANDT, SLCHD-NW-RS
ATTN L. LIBELO, SLCHD-NW-RS
ATTN A. BABA, SLCHD-NW-TN
ATTN L. BELLIVEAU, SLCHD-NW-TN
ATTN W. SHVODIAN, SLCHD-ST-AR
ATTN G. PISANE, SLCHD-ST-MW
ATTN J. DAVID, SLCHD-ST-R
ATTN A. KENDALL, SLCHD-ST-R
ATTN P. ALEXANDER, SLCHD-ST-SA
ATTN C. ARSEM, SLCHD-ST-SA
ATTN H. LE, SLCHD-ST-SA
ATTN D. WONG, SLCHD-ST-SA
ATTN R. GOODMAN, SLCHD-TA-ES
ATTN A. STEWART, SLCHD-V
ATTN T. WHITE, SMSLD-AS-SA
ATTN H. HARRELSON, SLCSM-AT
ATTN J. ORSEGA, SLCSM-GS
ATTN A. GLUCKMAN, SLCHD-NW-TN (5 COPIES)